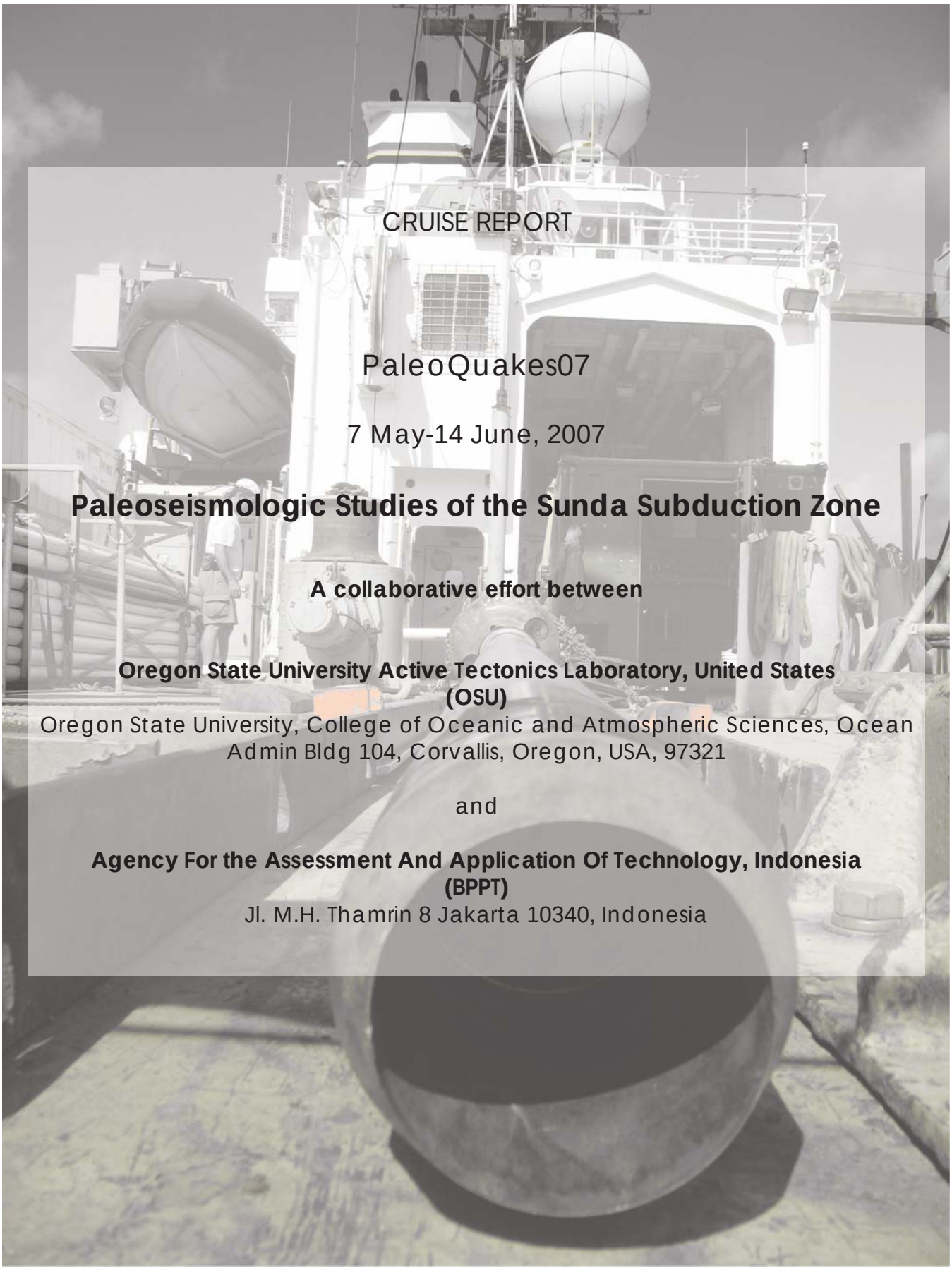

CRUISE REPORT

PaleoQuakes07

7 May-14 June, 2007

Paleoseismologic Studies of the Sunda Subduction Zone

A collaborative effort between

Oregon State University Active Tectonics Laboratory, United States (OSU)
Oregon State University, College of Oceanic and Atmospheric Sciences, Ocean Admin Bldg 104, Corvallis, Oregon, USA, 97321

and

Agency For the Assessment And Application Of Technology, Indonesia (BPPT)
Jl. M.H. Thamrin 8 Jakarta 10340, Indonesia

Acknowledgements

We gratefully acknowledge support from the Ocean Sciences and Earth Sciences Divisions of the US National Science Foundation, as well as the facilities division of NSF for providing science and equipment support for the project. We acknowledge our Indonesian partners let by Dr. Yusuf Djadjadihardja of BPPT.

This project could not have been done without close collaboration with colleagues at NOC,S, IFREMER, and BGR who provided critical bathymetric and sub-bottom profile data. These data allowed our project to proceed directly to site selection, with very little bathymetric survey required.

We gratefully acknowledge the professionalism and determination of the Captain, Mates, and crew of the R/V Roger Revelle and the Scripps Institution of Oceanography. Through the long process of establishing clearance and logistics for this cruise, the Scripps ship schedulers solved numerous problems large and small.

At sea, significant breakdowns aboard the Revelle involving winch and wire systems led to devising innovative workarounds that kept the ship operating and data and cores coming in against the odds. Captain Tom DesJardins and Chief Engineer Danny Mitchell were instrumental in this effort.

We acknowledge our Spanish partners from Unitat de Technologia Marina, CSICCentre Mediterrani d'Investigacions Marines I Ambientals (CMIMA), Barcelona, Spain. We appreciate the assistance of graduate students supported by Eulalia Gracia Mont. We are grateful for their participation.

We thank Bob Wilson for his long experience long hours, and knowledge of ships systems and handling gear without which coring might have ceased after a short time at sea. We also thank coring technicians Chris Moser, Paul Walszak and Kurt Shultz for their hard work and talents under the blistering equatorial sun. We also acknowledge the support of National Oceanography Centre, Southhampton for providing support for the participation of Russel Wynn, to BGR in Germany for supporting the participation of Stefan Ladage, and to AIST/GSJ in Japan for support for the participation of Ken Ikehara.

Table of Contents

Acknowledgements i
Table of Contents ii

I. Planning and Organization 1
a. Crew Names 1
b. Equipment 2
c. Geologic Background 3
d. Turbidite Methodology 4
i. Triggering Mechanisms 6
ii. Synchronous Triggering, Relative Age Control, and Regional Correlations 7
iii. Cascadia Results 9
iv. Northern San Andreas Fault 11
v. December 26th Earthquake 11
vi. Sumatra Regional Setting 14
vii. Seismogenic & Wedge Structure and Geometry 15
viii. Continental Margin Morphology and Sedimentation 19
1. Channel Systems 20
2. Foram Abundance 20
3. Margin Physiography 21
ix. Coring Approach 21
x. Objectives 22
II. Cruise Synopsis 23
a. Core Siting 23
b. Age Control 25
c. Physical Property Correlation 26
d. Ash Stratigraphy 27
III. Summary of Results 27
a. Lithology and Sediment Sourcing 28
b. Sites 29
IV. Cruise Narrative 38
V. References 33
VI. Appendices 33
a. Appendix 1. Memorandum of Understanding A-1-1
b. Appendix 2. Site Maps, (plan view) A-2-1
c. Appendix 3. Site Maps, (oblique view) A-3-1
d. Appendix 4. Sample Core Logs A-4-1
e. Appendix 5. KNOX05RR Trackline Map A-5-1
f. Appendix 6. Core Location Map (D-sheet) ..... (on cd-rom)

This Page Intentionally
Left Blank

Project Planning and Organization

The PaleoQuakes07 project is a collaboration between Oregon State University, and the Agency for the Assessment and Application of Technology (BPPT) in Indonesia. The US Chief Scientist was Dr. Chris Goldfinger of Oregon State University, and the Chief Indonesian Scientist was Dr., Yusuf S. Djajadihardja. The cruise involved invited participation by NOC,S (Great Britain), BGR (Germany) AIST (Japan) and LIPI in Indonesia. The cruise was carried out under the auspices of a Multihazard Memorandum of Understanding between the United States and Indonesia signed November 20, 2006 in Jakarta by State Minister for Research and Technology Kusmayanto Kadiman for the government of the Republic of Indonesia and Ambassador B. Lynn Pascoe for the United States (**Appendix 1**). The MOU covered activities from geologic research to tsunami warning systems and extends from the date of signing for five years.

The cruise consisted of two legs, with a port call in Pandang, west Sumatra of one day, with an exchange of several science party members. The science party roster and affiliations are shown in **Table 1**.

Table 1. Cruise Participants for Paleoquakes07.

	Name		Nationality
SCIENCE PARTY:			
1	Chris Goldfinger	M	US
2	Joseph Stephen Stoner	M	US
3	Ann Elizabeth Morey Ross	F	US
4	Jason Robert Patton	M	US
5	Christopher Glenn Romsos	M	US
6	Maureen Helen Davies	F	US
7	Javier Moncada	M	US
8	Nathan David Potter	M	US
9	Bart J. M. DeBaere	M	Belgium
1	Yusuf Djadjadihardja	M	Indonesia
2	Udrekh Hanifa	M	Indonesia
3	Sapta Chahyadi Sahputra	M	Indonesia
4	Nanang Hadi Prabowo	M	Indonesia
5	Eddy Zulkarnaen Gaffar	M	Indonesia
8	Yudo Haryadi	M	Indonesia
9	Sri Ardhyastuti	F	Indonesia
10	Riza Rahardiawan	M	Indonesia
11	Dayuf Jusuf	M	Indonesia
20	Ximena Moreno Mota	F	Spain
21	Elena Pinero Melgar	F	Spain
22	Alexis Vizcaino Marti	M	Spain
23	Oriol Pigue Serra	M	Spain
24	Zoraida Rosello Espuny	F	Spain
25	Russell Barry Wynn	M	UK
26	Eugene Charles Morgan	M	US
27	Ken Ikehara	M	Japan
28	Stefan Ladage	M	Germany
29	Christopher David Aikenhead	M	Canada

	Name		Nationality
CORING TECHNICIANS:			
30	John Christian Moser	M	US
31	Robert Clay Wilson	M	US
32	Paul Steven Walczak	M	US
33	Kurt William Schultz	M	US
34	Roberto Gonzalez Alvarez	M	Spain
35	Ramon Ametller Torres	M	Spain

Equipment Employed in the PaleoQuakes07 Project

The vessel R/V Roger Revelle is equipped with a Simrad EM-120 multibeam sonar system capable of mapping to full ocean depths. This system was used extensively to map portions of the continental slope and adjacent abyssal plain to fill areas not previously mapped, and to map channel systems poorly imaged in previous surveys. Daily XBT's were done to establish water velocity profiles for correcting depths, and tide corrections were subsequently applied to the multibeam data. The Simrad EM-120 data were processed with MB System software, and visualized at sea using IVS Fledermaus and ESRI ArcGIS 9.2 software. Bathymetry as well as backscatter and sidescan mosaics were processed from the Simrad data.

The ship is also equipped with a Knudsen model 320B/R 3.5 kHz chirp sub-bottom profiler used both to image seafloor sediment character, and to track the acoustic pinger attached to most coring systems as an aid to approaching the bottom. In profile mode in either 12 KhZ or 3.5 kHz modes, the profiler can sweep from, 0.18-24 ms. In 12 kHz mode, the system was used to track a 12 kHz pinger placed typically 75 above the coring device. These data were recorded digitally in SEGY format and also in the Knudsen native KEB playback format.

OSU supplied coring gear for the project including two complete 4" Jumbo piston coring systems, one jumbo gravity corer, one Ocean Instruments 8 tube multicorer, one small diameter benthos gravity corer, and two jumbo kasten corers 21cm square by 3m in length. The piston corers were supplied with shock absorbing pistons of new design to prevent wire breakage from pre-tripping, and from other shock loads (**Figure 1**). These shock-absorbing pistons were developed to extend the capabilities of the

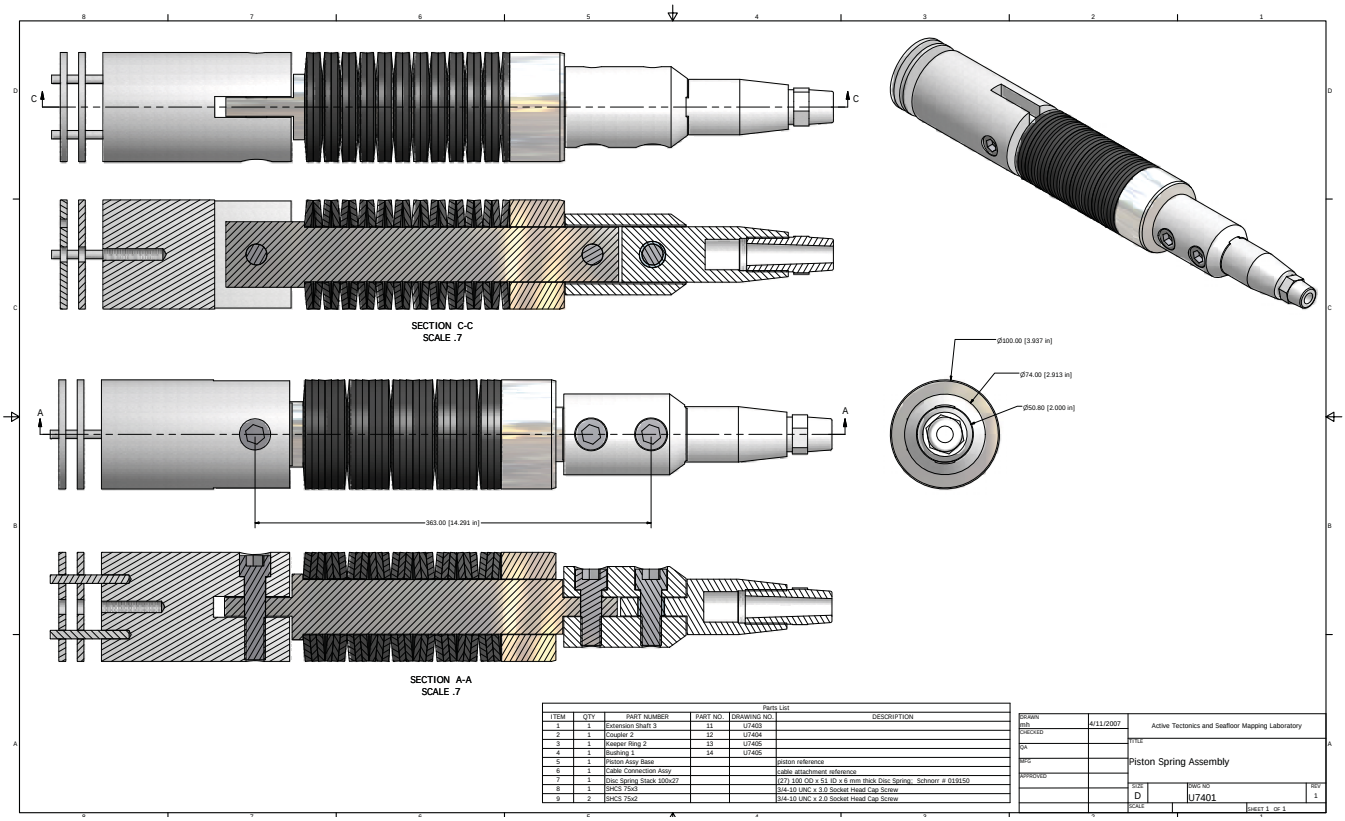

Figure 1. Shock absorbing piston using disc springs to reduce shock loads during pre-trip or over early tripping of the corer in very deep water. Designed by OSU active Tectonics lab, patent applied for.

small 9/16 wire used on US vessels, which is near it's elastic limits when coring in 5000-6000m of water as in this project in the Sunda Trench.

The ship routinely collected ADCP, gravity, salinity, temperature, meterorological, surface water velocity, oxygen, and depth data.

Navigation for all surveys and sites was with P-Code or differential GPS with typical position errors of 2-5m.

Geologic Background

Subduction earthquakes represent one of the largest releases of energy on earth, and the December 26th 2004 Sumatran earthquake is the second or third largest earthquake ever recorded (**Figure 2**). Quantifying the temporal and spatial patterns of these great events remains elusive because our observations span too little time to encompass more than a few seismic cycles, and because the ability to directly measure the associated accumulation and dissipation of strain energy has only recently been developed. GPS technology now makes it possible to measure elastic strain accumulation at plate boundaries with a high precision in only a few years. However, real-time strain measurements can only represent a fraction of one strain cycle. Fundamental questions such as the utility of the seismic gap hypothesis, clustering, and the applicability of slip-predicable or time-predicable models remain unanswered because we rarely have a long enough earthquake record. Paleoseismology addresses these questions directly using a larger time span than available to geodesists. The use of paleoseismology in subduction settings is now advancing rapidly. In the past decade, discovery of rapidly buried marsh deposits and associated tsunami sands along the Pacific Coast of the US Pacific Northwest has led to the recognition that the Cascadia subduction zone, once thought aseismic, has generated great (Mw 8-9) earthquakes in the past. The questions of how large and how frequent these events are, and their spatial and temporal distribution are now the active areas of research in Cascadia and elsewhere.

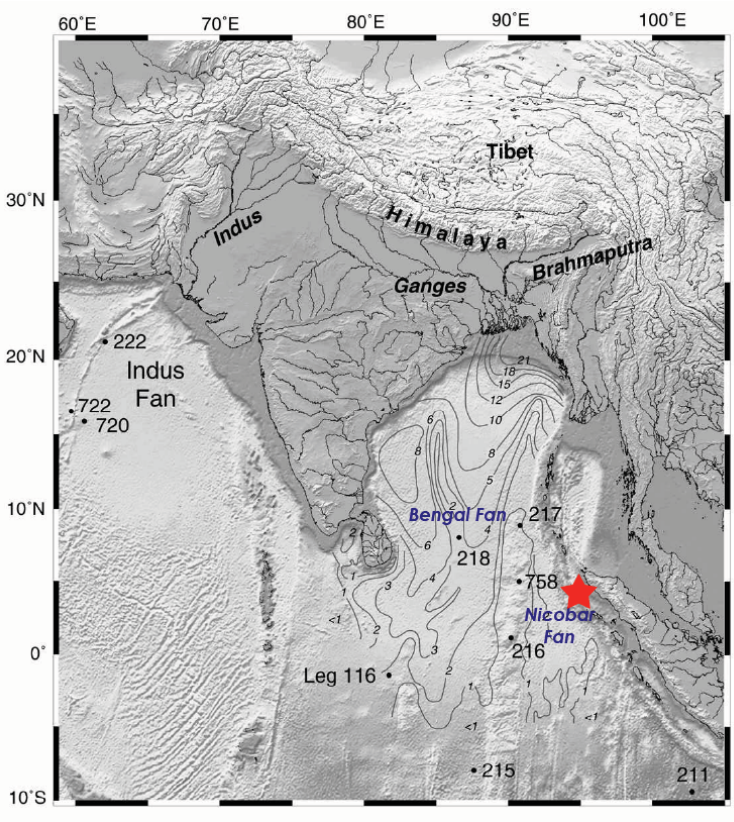

Figure 2. *Map of the Himalayan/Indian Ocean region showing the mainshock of the 26 December Mw 9.3 Sumatran earthquake. Positions of DSDP and ODP Sites are also shown. Isopachs (km) of the Bengal and Nicobar Fans are shown. From France-Lanord et al., 2000.*

At active continental margins off fault paleoseismologic techniques are being developed. Off fault techniques must demonstrate that the geologically recorded

events are uniquely generated by earthquakes and not some other natural phenomenon. These problems can be overcome, and the techniques can be powerful tools that offer in many cases, very long seismic time series. Coastal marsh paleoseismology has defined the Cascadia record, and is now being used in the Japan, Nankai, Kurile, Alaskan, and Chilean subduction systems. These records can define the record over the past 1000-3000 years typically, with scattered longer records. The marine sedimentary record contains a long and uninterrupted turbidite record extending back as much as ~10,000 years (and much longer), more than enough to encompass many earthquake cycles. In recent years, turbidite paleoseismology has been attempted in Cascadia (Adams, 1990; Goldfinger et al., 2003 a, b, 2004; Nelson et al., 1996; Nelson et al., 2000a), Japan (Inouchi et al., 1996; Shiki et al., 2000; Nakajima et al., 2004; Noda, 2004; Okamura, 2004; Soh, 2004), the Mediterranean (Kastens, 1984; Nelson et al., 1995), the Dead Sea (Niemi and Ben-Avraham, 1994), northern California (Field et al., 1982; Garfield et al., 1994) the Arctic ocean (Grantz et al., 1996), and several inland lakes (Karlin and Abella, 1992; Karlin et al., 2004; Smoot et al., 2000; Kumon et al., 1998; Schnellman et al., 2002). We have been successful in advancing knowledge of Cascadia subduction earthquakes using the turbidite paleoseismologic record, and are currently completing final manuscripts (Goldfinger et al, 2003a,b; 2004; 2005 submitted). We are also completing an investigation of the turbidite history along the San Andreas Fault in Northern California. We now propose to apply these methods to the turbidite history along the Sumatra margin, where the great earthquake of December 26, 2004 struck. The physiography and sedimentation of the Sumatra-Nicobar-Andaman section of the trench is quite similar to the nearly ideal Cascadia margin, and presents a good opportunity to adapt the technique. In the next sections we discuss our results from Cascadia, the northern San Andreas, and Japan to substantiate the methods we propose to adapt to Sumatra. Lastly, continued development of the turbidite paleoseismic technique advances fundamental tectonic and seismic hazard methods that can be applied in any continental margin system, where major fault systems and population centers commonly coincide.

Turbidite Methodology and Application to Cascadia and the San Andreas

Following the discovery of the first buried marsh sequences on land, Adams (1990) used existing cores to test the possibility that the Cascadia cores contained a record of Holocene great earthquakes of the Cascadia margin. Fortunately, Oregon and Washington cores all contain a unique datable event, the ash layer from the eruption of Mount Mazama, at 7627 ± 150 cal yr BP (Zdanowicz et al., 1999). The ash was distributed to the channel system via the drainage basins of major rivers. Only channel cores contain the ash, indicating that airfall offshore was not significant.

Adams (1990) examined core logs for Cascadia Basin cores, and determined that nearly all of them had 13 turbidites overlying the Mazama ash, and argued that these 13 turbidites correlate along the channel. Adams observed that cores from Juan de Fuca Canyon, and below the confluence of Willapa, Grays, and Quinault Canyons, contain 14-16 turbidites above the Mazama ash. The correlative turbidites in Cascadia channel lie downstream of the confluence of these channels. If these events had been independently triggered events with more than a few hours separation in time, the channels below the confluence should contain the sum of the tributaries, from 26-

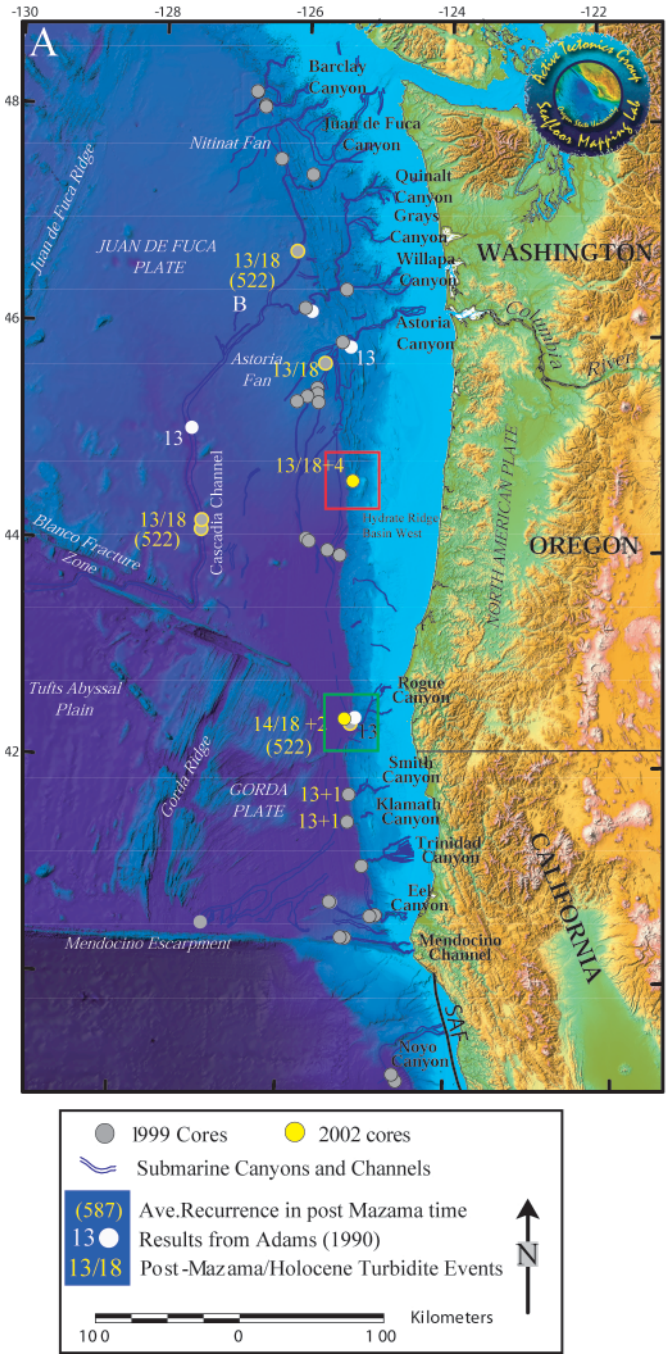

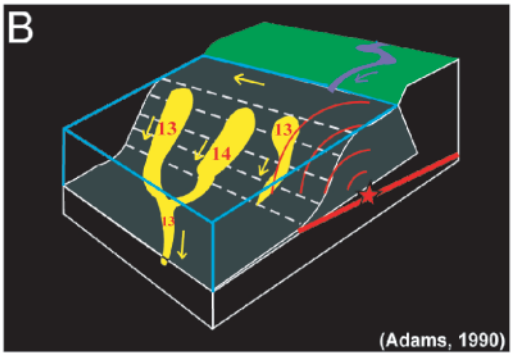

Figure 3. A. Cascadia margin turbidite canyons, channels and 1999-2002 core locations. Major canyon systems are outlined in blue. Number of post-Mazama and/ or Holocene correlative turbidites as well as the average Holocene recurrence time are shown in yellow. Mazama ash was not present in Barclay Canyon cores or in the cores south of Rogue Canyon. Primary core sites shown with yellow rim, other cores are grey. Remarkable similarity of records in Cascadia suggests a central rupture segment with a minimum of 700 km length that has ruptured 19 times during the Holocene. Two events, T5 and T5a ruptured southern and northern segments respectively, although considerable overlap probably existed. 13 local events in southern Oregon not shown. Green square shows new 2002 Rogue core RR0702-55KC. Red square shows new Hydrate Ridge (HR) basin site, and core RR0702-56PC. No Mazama ash is found at HR, but physical correlation identifies the margin wide event that bears channel delivered ash elsewhere.
B. Synchroneity test at a channel confluence as applied where Washington channels merge into the Cascadia Deep Sea Channel. The number of events downstream should be the sum of events in the tributaries, unless the turbidity currents were triggered simultaneously by an earthquake (Adams, 1990). This site is at "B" on the JDF plate.

31 turbidites, not 13 as observed (**Figure 3**). The importance of this simple observation is that it demonstrates synchronous triggering of turbidite events in tributaries, the headwaters of which are separated by 50-150 km. This elegant relative dating technique is used extensively in our Cascadia and SAF work.

Using 54 new cores in Cascadia, we have confirmed and extended the event record temporally and spatially. Because one event does not correlate the length of the margin, there are actually 14 post-Mazama and 19 Holocene events along~ 660 km of the margin in the Cascadia, Barclay, Willapa, Grays, and Rogue Canyon/ Channel systems between latitudes 42N and 48N (**Figure 3**). The most recent event took place in 1700 AD (Satake et al., 1996; Nelson et al., 1995), and an additional 18 turbidite events have occurred during the preceeding9750 years, yielding a mean recurrence time of ~525 years. Several four other smaller events are correlated over short distances.

Triggering Mechanisms: Are They Earthquakes?

Are these events all triggered by earthquakes? Common sense suggests that such a scenario is absurdly simplistic, yet our Cascadia work has led us to the unlikely conclusion that Adams (1990) was correct. We now discuss the methods used to test the hypothesis and why it seems to work. Adams (1990) suggested four plausible mechanisms for turbid flow triggering: 1) storm wave loading; 2) great earthquakes; 3) tsunamis; and 4) sediment loading. To these we add 5) crustal earthquakes, 6) slab earthquakes, 7) hyperpycnal flow, and 8) gas hydrate destabilization. All of these mechanisms can and do trigger a turbidity currents, but how often do they actually occur, and can earthquake-triggered events be distinguished from other events? Two techniques can distinguish seismic from non seismic events:

1) Sedimentological determination of individual event origin.
2) Regional correlations that require synchronous (i.e. earthquake) triggering.

Individual event determination can in some cases distinguish seismic turbidites from storm, tsunami, and other deposits using several methods. Nakajima and Kanai (2000) and Shiki et al. (2000) report that seismo-turbidites can in some cases be distinguished sedimentologically. They observe that historically known seismically derived turbidites in the Japan Sea and Lake Biwa are distinguished by wide areal extent, multiple coarse fraction pulses, variable provenance, and greater depositional volume than storm-generated events. These investigators traced known seismo-turbidites to multiple slump events in many parts of a canyon system, generating multiple pulses in an amalgamated turbidity current, some of which sampled different lithologies that are separable in the turbidite deposit. In general, these investigators observe that known storm triggered events are thinner, finer grained and have simple normally graded Bouma sequences, although complexity is also a function of proximity to the source, and some reports reach different conclusions (Mulder and Syvitski, 1996). While there may be global, regional or local criteria to make such distinctions, these are at present poorly developed and somewhat contradictory.

Thus far in Cascadia and along the San Andreas system, we have not attempted to distinguish between triggering mechanisms directly because the physiography, numerous tephra layers, and long historical records favorable to this method in Japan are not present on the US west coast. Determination of synchronous triggering can eliminate non-earthquake triggers with the possible exception of storm wave loading or multiple hyperpycnal flows for very large storms. West Coast physiography favors filtering of non-seismic events from the record because a wide shelf separates river sources from canyon heads. Hyperpycnal flow, or direct turbid injection from rivers, can produce turbid flows, and can even mimic earthquakes in that they may affect several rivers over a span of days. We have found that while this certainly occurred during the Pleistocene when lowered sea-level resulted in direct river-canyon connections, during high stand conditions this does not occur (e.g. Sternberg, 1986). Two exceptions are the Eel river record, which probably contains storm events, and the Viscaino channel along the northern San Andreas. Both channels head at a very narrow shelf, and river injection is possible. Deep canyon heads also prevent triggering by storm wave loading and distant tsunami, the last two non-earthquake sources. For example, in Cascadia, where, although deep water storm waves are

large, the canyon heads where sediment accumulation occurs are at water depths of 150-400 m, too deep for disturbance by maximal storm waves of ~20 meters. Tsunamis may also conceivably act as a regional trigger, however the tsunami from the 1964 Alaska Mw 9.0 event did not trigger a turbidite observed in any of the cores. Crustal or slab earthquakes could also trigger slumps and turbid flows, though not regionally. To test for this, in 1999 we resampled the location of a 1986 box core in Mendocino channel, where the uppermost event is suspected to be the 1906 San Andreas earthquake. The Mw7.1 Petrolia earthquake occurred in 1992 at this location, with an epicentral distance of only a few km from the canyon head. We found no turbidite in the 1999 box core, suggesting that triggering at that site may require earthquakes larger than Mw 7.2. Conversely, the Loma Prieta earthquake apparently did trigger a turbid flow event in Monterey Canyon at a greater epicentral distance (Garfield et al., 1994), though it is not known whether a discernable turbidite record exists from this event. Japanese investigators have suggested a minimum magnitude of ~ Mw=7.2 for turbidite triggering, though we suspect that this minimum value is site and event specific.

Synchronous Triggering, Relative Dating, and Regional Correlations

Taking advantage of favorable physiography, we have used spatial and temporal patterns of event correlations that are unlikely be the result of triggers *other* than earthquakes. We use multiple techniques to test for linkage between specific events, and thus test for synchroneity. Typically, paleoseismologic investigations use radiocarbon constraints to establish these linkages, but often are unable to determine synchronous event chronology due to the inherent limits in dating techniques. Relative dating techniques, if available, and if of sufficient resolution, are strongly preferred to test for synchroneity. The "confluence test" of Adams (1990) is powerful in that it requires synchronous triggering within a few hours. Comparisons of numbers of events between time markers is a somewhat less powerful technique that can be useful. Recently we have begun to use direct physical property correlations, which are proving to be a powerful new method of testing for linkages (if present) between sites. We have found that it is possible to correlate the physical property signatures of individual turbidites from locale to locale down individual channels (**Figure 4**). This indicates that the details of the turbid flow that are relevant to deposition of the turbidite apparently maintain their integrity for long distances within channels. This in itself is quite surprising, and offers the opportunity to use these direct correlations to extend and strengthen the turbidite event stratigraphy. What is more surprising is that we have been able to correlate event signatures not only down individual channels, but between channel systems that never meet. Our current working hypothesis is that the coarse pulses represented in the magnetic and density "fingerprints" of individual events could represent some source characteristic of the triggering earthquake. For example, the Great Sumatran earthquake had three separate subevents, four if the long slow northern section is considered. Our model would predict that these subevents, minutes apart, may be recorded as discernable coarse pulses within the turbidite that can be correlated over distances. A simple experiment in our lab has demonstrated that this mechanism can work, with pulse separation of as little as 1 second (Goldfinger et al., 2004). We also see a general correspondence of turbidite size and character that is reflected in these separate channels, as well as correlatable

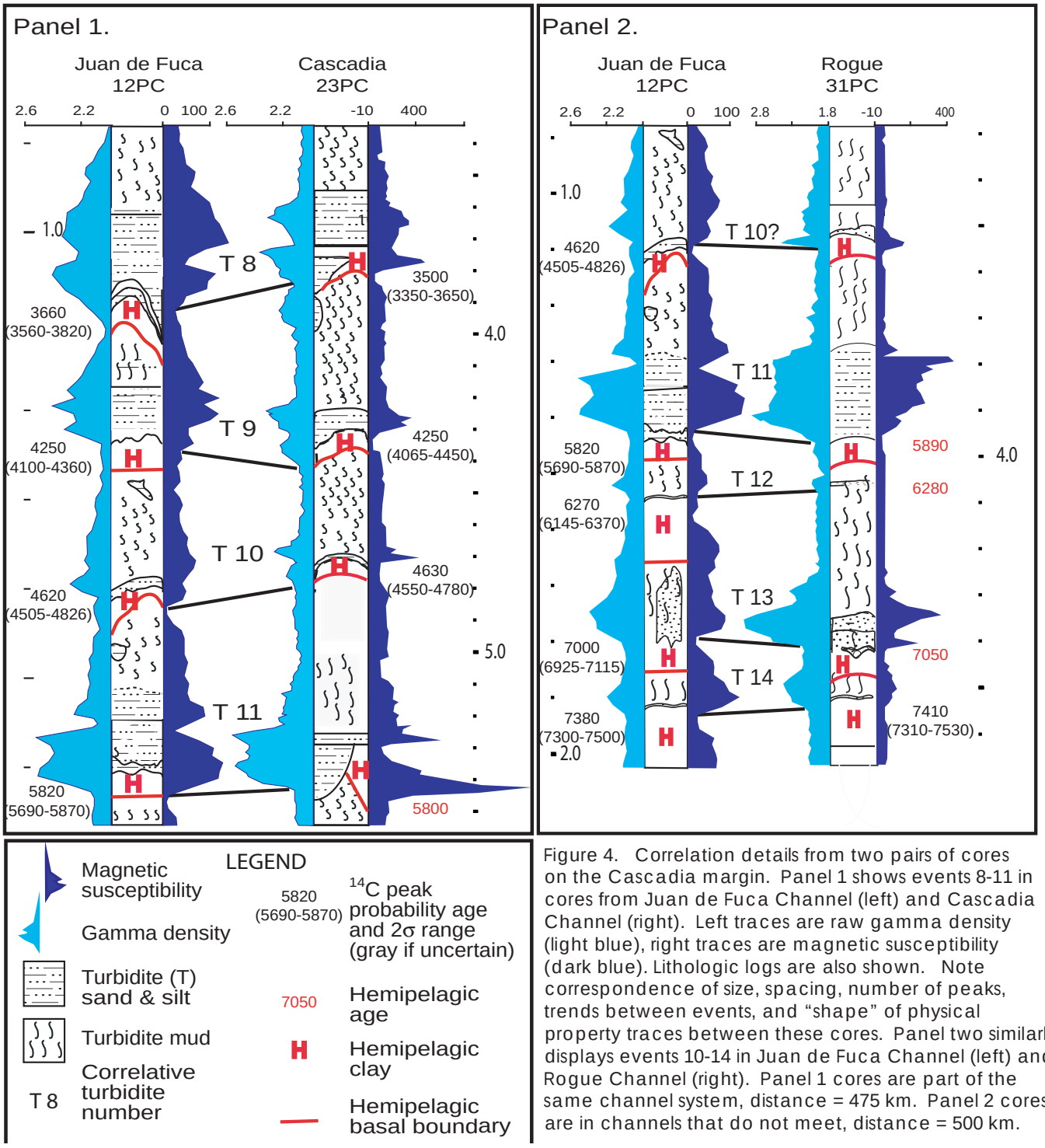

Figure 4. Correlation details from two pairs of cores on the Cascadia margin. Panel 1 shows events 8-11 in cores from Juan de Fuca Channel (left) and Cascadia Channel (right). Left traces are raw gamma density (light blue), right traces are magnetic susceptibility (dark blue). Lithologic logs are also shown. Note correspondence of size, spacing, number of peaks, trends between events, and "shape" of physical property traces between these cores. Panel two similarly displays events 10-14 in Juan de Fuca Channel (left) and Rogue Channel (right). Panel 1 cores are part of the same channel system, distance = 475 km. Panel 2 cores are in channels that do not meet, distance = 500 km.

details such as the number of coarse pulses (density and magnetic peaks). For example, in **Figure 4** events T5, T10, and T12 are small events in all cores at all sites. T11 and T16 are very large events in all cores, and most other events follow similar size patterns across the margin. This information suggests that there may be some fundamental relationship to the underlying earthquakes, or alternatively perhaps to sedimentation events. The underlying reasons for this are at present unclear, and are under investigation in our Cascadia and SAF work. Nevertheless, though the

explanation is pending, we have been able to use these persistent characteristics to build a correlation method. Physical property correlations are common practice with ODP cores, in the oil industry, and have recently come into use for paleoseismology (i.e. Abeldayem et al., 2003; St-Onge et al., 2003; Hagstrum et al., 2004, Iwaki et al., 2004; Karlin et al., 2004, Schnellmann et al., 2002). Turbidite "fingerprints" have been recognized and used for regional correlation in Lake Baikal (Lees et al., 1998), off Morocco (Wynn et al., 2002), and elsewhere.

Cascadia Results

Using Adams' "confluence test", we originally concluded that the northern Cascadia margin contained 18 Holocene events, all of which pass this test of synchronous triggering. The southern Oregon Rogue site, also contains a record of 18 Holocene and 13 post Mazama events, though Rogue channel has no confluence with the other systems (**Figure 3**). It passes a weaker test by virtue of having an identical number of events to the northern margin (Goldfinger et al., 2003a,b). Subsequent to these results, we have found it possible to correlate the 18 Holocene events directly using physical properties of the turbidites themselves in the cores. One event proved to be segmented, yielding a total of 19 major events. Four other smaller events have occurred only along the southern Oregon margin (**Figure 3**). Using these correlations we believe it is possible to establish synchronous triggering for the northern and central parts of the margin between 42 and 48 degrees N (**Figure 3**) for 18 events, with one "extra" event divided between two segments. In Cascadia, event synchroneity is established not only with radiocarbon ages, but with correlation techniques within a radiocarbon constrained framework. Correlations now link northern and southern sites, a connection that radiocarbon evidence alone cannot establish with either onshore or offshore records. **Figure 5** illustrate the correlation between sites 500 km and 375 km apart respectively using joint ash, biostratigraphic, radiocarbon, and physical property correlation.

Figure 5 shows results of radiocarbon ages from our three key core sites in Cascadia, at Juan de Fuca, Cascadia, and Rogue Channels along with published land paleoseismic data, plotted against latitude along strike. The plot shows 18 margin-wide events one large segmented event, and four smaller events that have been jointly correlated with physical properties and radiocarbon ages. Published land ages are also included in this plot. This plot suggests clustering of events in time through much of the Holocene. During this period, we observe five long intervals between clusters of events with an average periodicity of ~1500 years. Between these long intervals, we see 2-5 shorter intervals. The smaller correlated events seem to partially fill some of the long gaps. Remarkably, this pattern is quite robust in both land and offshore data, and not likely to be coincidental, even though individual event ages may or may not overlap at the 1 or 2 sigma level (Goldfinger et al., 2003a; 2003b) Some non-overlapping ages are well correlated with MST data.

The discovery of a possible repeating pattern among Cascadia Great earthquakes, if correct, offers opportunities that are rare in active fault research. We observe that clusters in the past 10,000 years have included 2-5 events, and the last event in AD 1700 was either the fourth event in the current cluster, or the fifth event if T5 is included, thus it is unclear whether the present cluster is concluded if five events is the maximum. Another alternative is that the very small T2 event was a "gap filling event". In that case, the ~ 600-700 year gap between T1 and T3 would imply that the AD1700 event

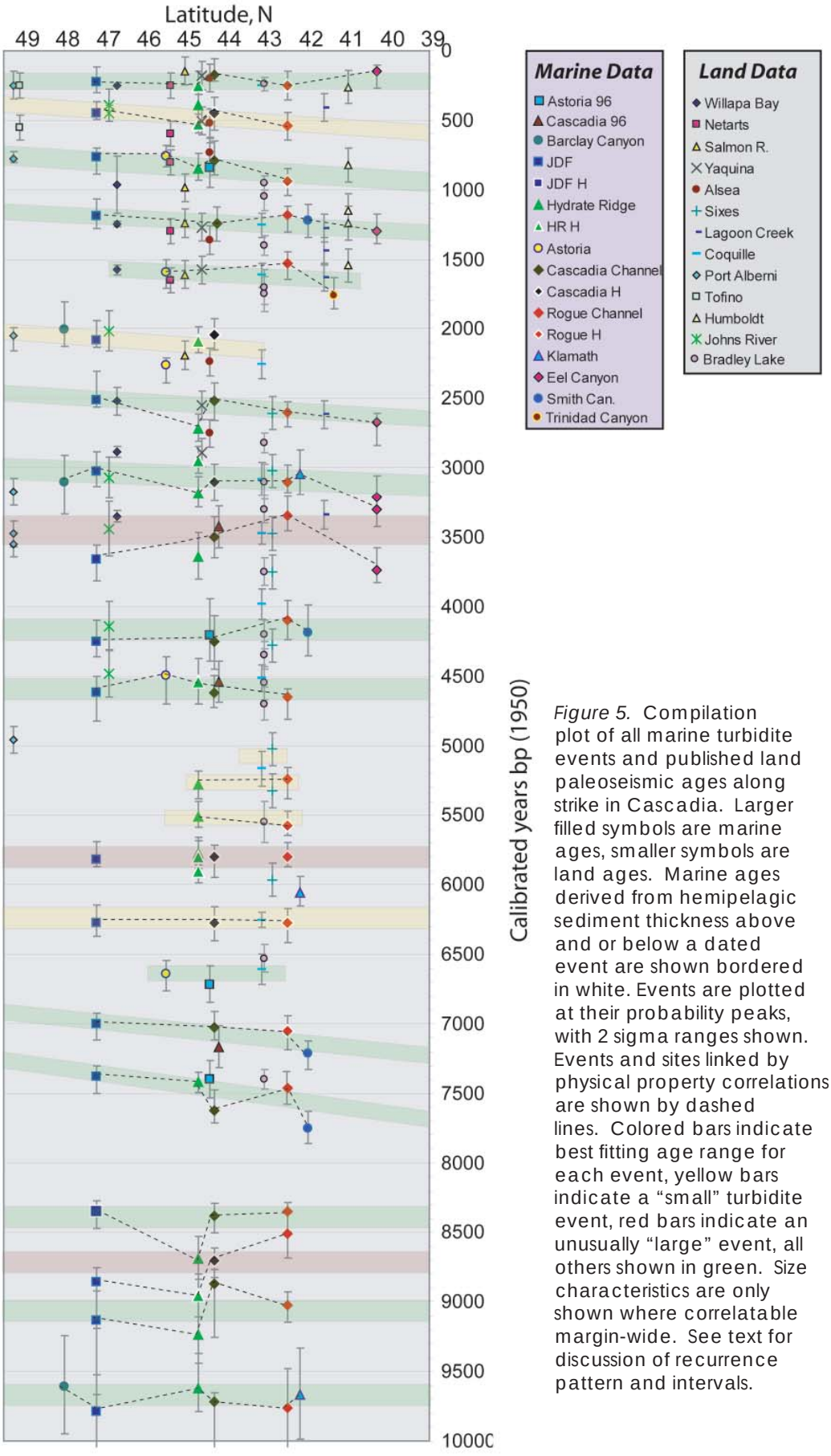

Figure 5. Compilation plot of all marine turbidite events and published land paleoseismic ages along strike in Cascadia. Larger filled symbols are marine ages, smaller symbols are land ages. Marine ages derived from hemipelagic sediment thickness above and or below a dated event are shown bordered in white. Events are plotted at their probability peaks, with 2 sigma ranges shown. Events and sites linked by physical property correlations are shown by dashed lines. Colored bars indicate best fitting age range for each event, yellow bars indicate a "small" turbidite event, red bars indicate an unusually "large" event, all others shown in green. Size characteristics are only shown where correlatable margin-wide. See text for discussion of recurrence pattern and intervals.

is the beginning of a new cluster, and Cascadia would be well within the range of repeat times for past clusters. Our results suggest these several possibilities for the future in Cascadia, if indeed the past can be considered representative of future fault behavior (Goldfinger et al. submitted).

Northern San Andreas Fault Turbidite Investigation

In 1999 and 2002, we collected 74 piston, gravity and jumbo Kasten cores from channel and canyon systems draining the northern California margin on the Scripps R/V Melville and R/V Roger Revelle. In our initial cores, we found thirty-one turbidite beds above the Holocene/Pleistocene faunal "datum" in Noyo Channel. Thus far, we have determined ages for 20 (of 38) events including the uppermost 5 events from cores 49PC/TC and adjacent box core 50BC using AMS methods. The uppermost event returns a "modern" age, which we interpret is likely the 1906 San Andreas earthquake. The hemipelagic age for this event is between 1892 and 1907 + 70, verifying the sedimentation rate and hemipelagic calculation. The penultimate event returns an intercept age of AD 1663 (2 sigma range 1505 - 1822). The third event age is AD 1524 (1445-1664). The fourth event age is AD 1304 (1057 - 1319), and the fifth event age is AD 1049 (981-1188). These early results are in good agreement with the onshore work to date which indicates an age for the penultimate event in the mid-1600's, the most likely age for the third event of ~ 1200-1300 AD. Our record contains 10 events in ~2500 years, while Niemi et al. (2002) also report 10 events during approximately the same period at the Vedanta paleoseismic site.

Our sampling program included all major and many minor channel systems extending from Cape Mendocino to just north of Monterey Bay. Sampling both down and across channels in some cases was done, and particular attention was paid to channel confluences, as these areas afford opportunities to test for synchronous triggering of turbidity currents. This project is ongoing as of this writing. We are continuing to develop the techniques learned in Cascadia to address the San Andreas margin. Thus far, we have found that physical property correlation is successful in this setting as well, and is consistent with the radiocarbon ages completed thus far. We have made extensive use of Adams' confluence test at the six major confluences available offshore northern California. We observe distinctive turbidite signatures from both heavy mineral assemblages and physical property signatures in individual channel systems merge at confluences into single turbidites that mix these characteristics into single turbidites downstream. The synchronous triggering of events is being established in this way, supported by a radiocarbon age framework.

Like Cascadia, we are also using a semi independent event chronostratigraphy based on the deposition of hemipelagic sediment between turbidites. The hemipelagic thickness can be plotted against radiocarbon ages to establish local sedimentation rate, and also to identify outliers in either radiocarbon ages or hemipelagic thickness, flagging possible basal erosion. Preliminary results from the SAF suggest that two segments may exist that sometimes rupture separately, and sometimes together, with the segment boundary located near a change in fault strike at Point Arena (Goldfinger et al., 2003b; 2004).

The Dec. 26th Great Sumatran Earthquake

On December 26, 2004, a magnitude ~9.2 earthquake struck Sumatra and the Andaman and Nicobar Islands of India (e.g., Park et al., 2005). Within hours, resulting tsunamis inundated coastal communities around the Indian Ocean, killing over 290,000 people. The earthquake ruptured the megathrust between the subducting India-Australia Plate and the overriding Burma-Sunda microplate (Fig. 1). Seismic rupture nucleated offshore Sumatra at ~30-40 km depth and ruptured mostly northwards for ~1300 km over a period of ~550 s (Lay et al., 2005; Ammon et al., 2005; Wu and Koketsu, 2005; Stein and Okal, 2005; Park et al., 2005). The December 26th earthquake was a surprise in many respects. That it occurred in a region thought to be quite poorly coupled was surprising. The initial estimates of magnitude were low, in the Mw8-8.5 range, however the tsunami demonstrated that the magnitude must have been much larger. Current energy estimates are in the Mw-9.2-9.3 range.

The initial models included a 400-450 km rupture with three sub events (**Figure 6**; Ammon et al., 2005) extending north from Simeulue Island. However it has become clear that the rupture continued for another ~ 800 km to the north, as indicated by the aftershock pattern and subsequent slip models (**Figure 6 and 7**). Additionally, tsunami modeling considering tide gauge data from eastern India and the travel times required requires that this northern rupture is needed to satisfy these data requires the rupture to extend to the Andaman Islands, consistent with the aftershock pattern.

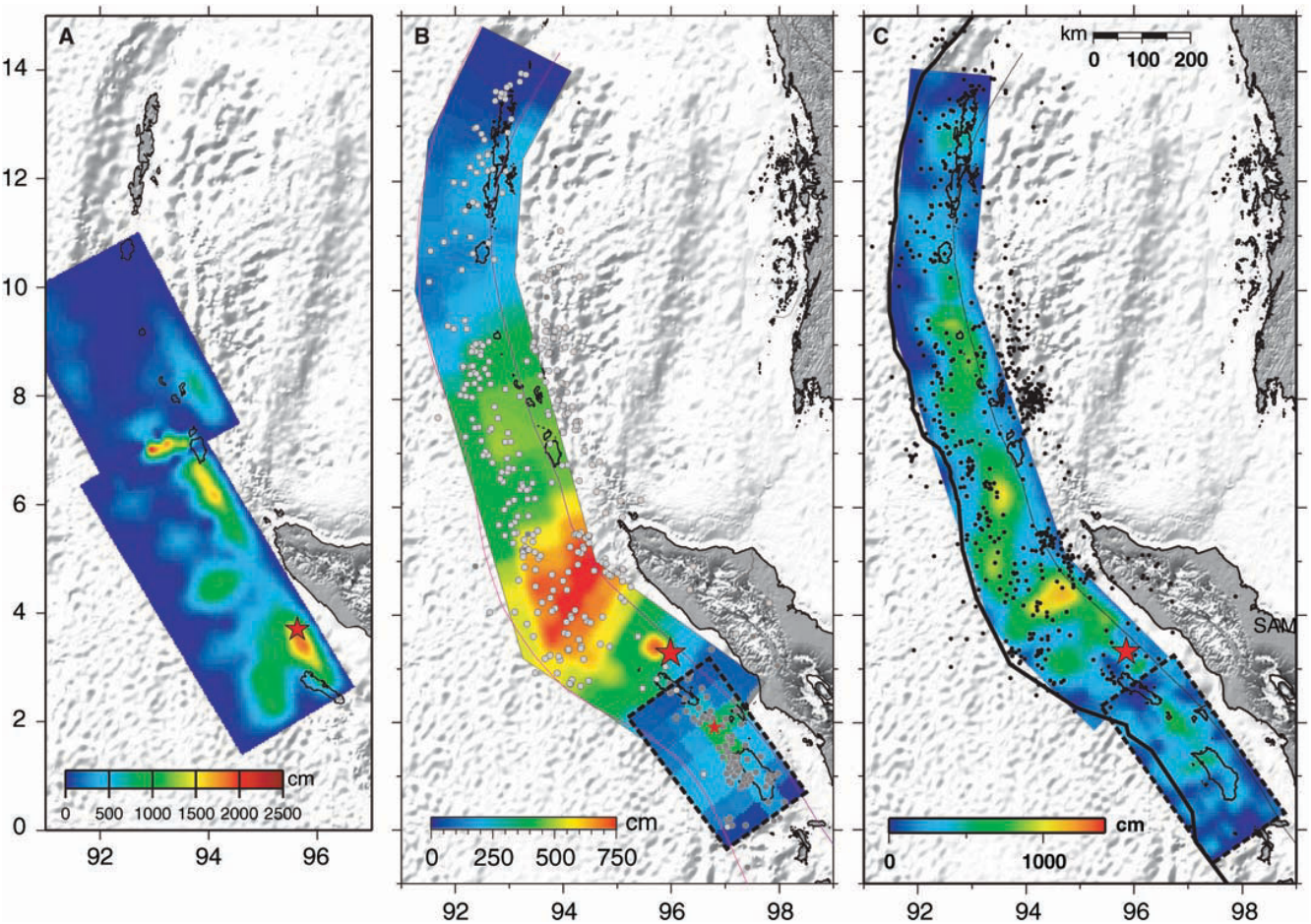

Figure 6. (A) Fault slip 168s after rupture initiation from teleseismic SH waveforms (B) Slip distribution of intermediate-period surface waves (C) Slip distribution using teleseismic body waves (5 to 200 s), int.-period three-component regional waves (50 to 500 s), and long-period teleseismic waves (250 to 2000 s). Fault segments colored by slip amplitude. After Ammon et al., 2005.

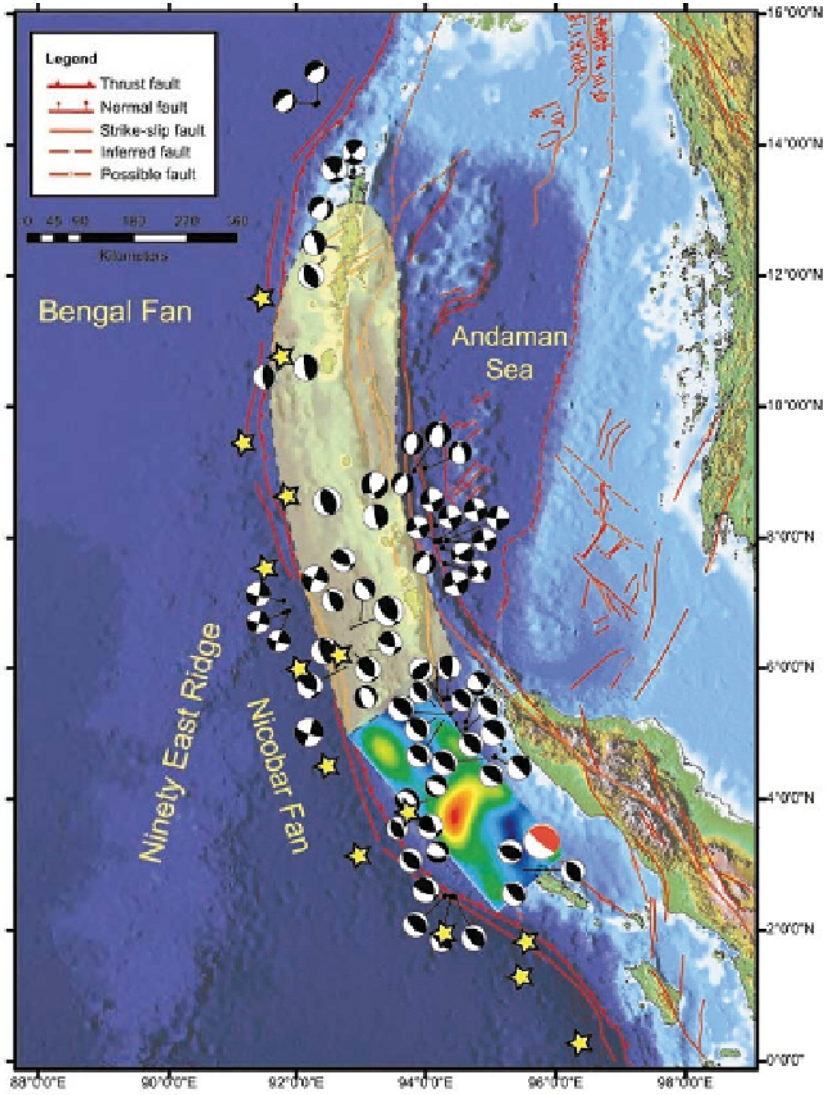

Figure 7. Rupture region of the 26 December 9.3 earthquake. Harvard focal mechanisms from the Harvard Catalog up to February 12, subsetted. Mainshock shown by red beachball. Rupture model from Chen Ji (Caltech) shown, showing three subevents. Tsunami models by NOAA and K. Satake require larger rupture to the Andaman Islands shown by shading. Faults from Curray et. al., in press. Proposed principal core sites shown as yellow stars, continued on Figure 8. Note clustering of aftershocks near the uplifted Island groups.

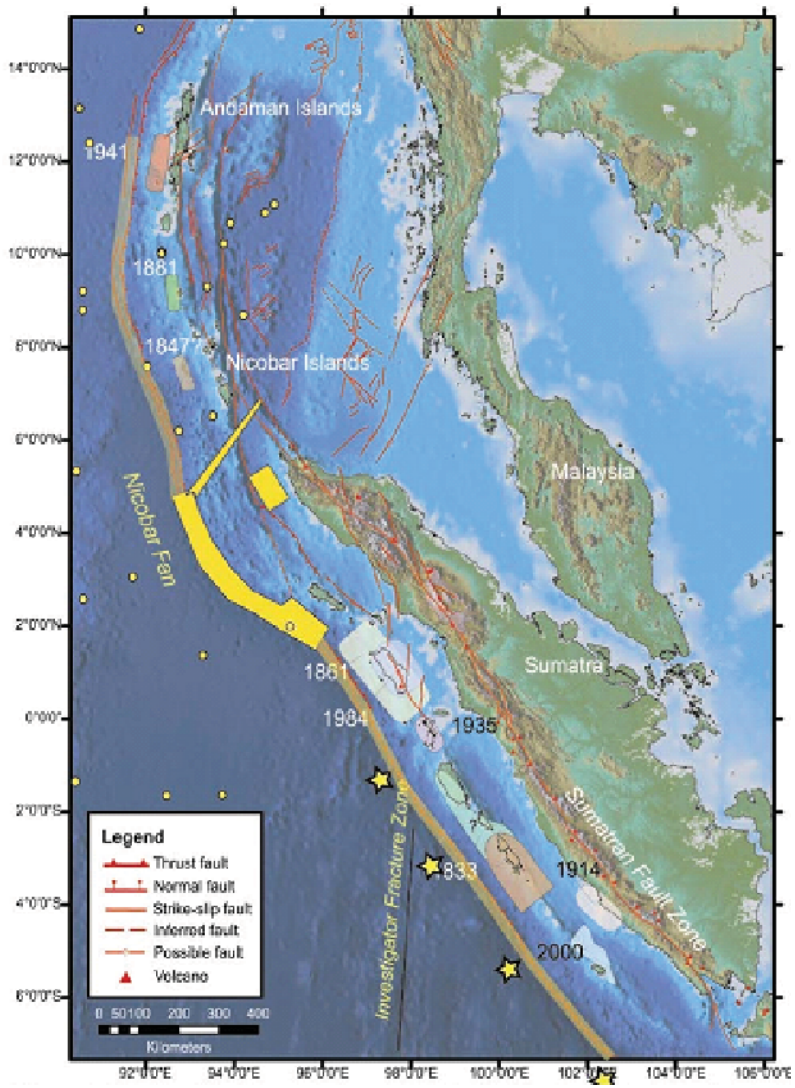

Figure 8. Sunda subduction zone form Jakarta to the Andamans showing known historical ruptures and paleoseismic record of Sieh et. al., 2000, Natawidjaja et. al., 2004 and references therein. Darker shaded rupture areas are found in the paleoseismic record. UK survey by HMS Scott shown in yellow, proposed survey shown in translucent yellow. Much of the proposed survey can be accomplished during inbound and outbound transits, as well as transits between core sites. Existing cores with foram abundance data shown as yellow dots.

The source time was ~ 350 seconds, almost six minutes. The northern rupture was very slow, and difficult to model from seismograms because of the very long period. The tsunami models may well be the most effective in capturing this earthquake source mechanism.

The tsunami was the most devastating event of its kind ever recorded. The subduction zone in the northern rupture area is unusual in that it is capable of generating waves in two directions, unhindered by land. The result was the enormous loss of life in countries both east and west of the mainshock. Coupled with the lack of knowledge of past earthquakes, and the lack of a tsunami warning system, the stage was set for the December 26th disaster.

Paleoseismic and historical evidence of past great earthquakes defines the ruptures of the past ~ 300 years very well. The precision record developed from the growth histories of microatolls by Kerry Sieh and students is unprecedented in it's precision, and it's ability to define vertical motion during paleoearthquakes. This record, though short, will be invaluable in calibrating the turbidite record we propose to collect (Sieh et al., 2000; Natawidjaja et al., 2003; 2004). Known ruptures along the Sunda trench are shown on **Figure 8**.

Sumatra Regional Setting

The Sunda trench results from the subduction of the oceanic Indo-Australian plate beneath the continental Burma Microplate (**Figure 1**). In the southern portion of the Sunda trench, convergence is directed towards the northeast, nearly normal to the margin, and the convergence rate decreases along the strike of the trench from 60 mm/yr off western Sumatra to ~ 50 mm/yr off the Andaman Nicobar margin (McCaffrey et al, 2000; Bock et al., 2003). From at least 0^0 to 14^0 the frontal thrust is intermittently landward vergent or shows no preferred vergence (shown in seismic profiles in Karig et al., 1980, Curray, 2006; and bathymetry and single channel profiles of Henstock et al., 2006 and Fisher et al., 2007). Southward from the equator, landward vergence is present but less common. In this region spanning the mainshock and extended rupture zone of the 2004 earthquake, the Nicobar Fan, a lobe of the larger Bengal Fan is being accreted and or subducted. The Ninetyeast Ridge physically separates the Nicobar and larger Bengal fan lobes, and is thought to have blocked sediment input to the trench from northern sources since the Pleistocene when it first intersected the Andaman margin (Curray, in press; **Figure 1**). Moore et al. (1976) report that a large Pleistocene submarine landslide also blocks the trench from northerly input at 14^0N. Incoming sediment thickness of the Nicobar fan is 2-4 km along the Andaman Nicobar region, thickening northward toward its former source to the north (Bandopadhyay and Bandyopadhyay, 1999).

Convergent margins in high sediment supply systems such as Sumatra typically comprise high accretion and fold growth rates in the youthful active prism, which represents only a part of margin history. The active wedge is commonly accreting outboard of an older prism and forearc basin complex. Most accretionary prisms are composed of imbricate landward-dipping (seaward-vergent) thrusts that accommodate rapid plate convergence. However, Sumatra, along with parts of Cascadia (e.g., MacKay et al., 1995; Goldfinger et al., 1996; Gulick et al, 1998, Adam et al., 2004), is one of a small number of prisms that also exhibit seaward-dipping or landward-vergent thrust faulting, (Henstock et al., 2006; Gaedicke et al., 2006a, 2006b; Fisher et al., 2007). The origins of the landward vergence are not yet clear,

and may be related to backstop geometry, accretion of overpressured fan sediments, or perhaps have other origins. In contrast to sequential accretion at most margins, the northern Sumatra forearc appears to deform in a different style: a steep outer wedge, and a steep descent into the Aceh forearc basin, are separated by a broad plateau (Henstock et al., 2006; Gaedicke et al., 2006; Fisher et al., 2007). Reflection data suggest that the trench sequence is thrust over a postulated duplex of older accreted material, possibly accounting for the flat topped forearc high (Ladage et al., 2006).

Like all convergent margins, the overall morphology of the Sumatra accretionary wedge can be controlled by many factors: vergence changes, changes in incoming sediment thickness over time, second order structures, contrasts in wedge strength, and variations in basal shear stress all contribute. Prism evolution is a dynamic process, and includes the long term geologic history as well as the evolutionary paths implied by general wedge taper models. These margin elements and processes all have potential links to the slip distribution and rupture propagation of great earthquakes. Despite extensive theoretical analysis of the causes of wedge taper changes, landward vergence in thrust belts, and links to décollement properties and seismogenesis, our knowledge is incomplete.

The forearc strike is arcuate, curving from NW near the Equator, to the north and then NE at 14^0 N. The obliquity of subduction also increases to the north, from near orthogonal at the Sunda Strait, to nearly pure strike-slip north of the Andaman Islands. Opening of the Andaman Sea backarc spreading center has added a local component of motion to the forearc region, maintaining an element of convergence along the trench even in the Andaman Islands region (Curray et al., 2006). The forearc is transported north and stretched as obliquity increases northward (Fitch, 1972; McCaffrey et al., 1991). Motion of the forearc sliver is accommodated by the Sumatran fault near the arc onshore, and also by strike slip faults such as the Mentawai and West Andaman faults in the submarine forearc (**Figure 8**; Sieh et al., 2000; Curray, 2006).

Pre 2004 GPS results from Sumatra and the offshore islands of the outer arc high strongly suggest a segment boundary between a southern strongly coupled segment, and a northern poorly coupled segment (McCaffrey et al., 2000; **Figure 9**). The boundary between the two segments lies near the north end of Siberut Island at ~ the equator. GPS vectors south of this point are close to parallel to the expected plate vector, indicating strong coupling of the forearc, while motion north of Siberut is nearly parallel to the arc, suggesting poor coupling and northward movement of the forearc sliver plate along the Sumatran fault, and also perhaps by strike-slip faults in the submarine forearc. The mainshock the December 26th earthquake occurred in the inferred poorly coupled region.

Relations Between the Seismogenic Zone and Wedge Structure/Geometry

Some sedimented accretionary systems show a sharp contrast in structural and geomorphic style between their seaward (lower slope) and landward (upper slope and outer arc high) parts (Figure 10). There are variations in wedge profile across each margin (e.g., Gulick et al., 2004), but most margins have key elements in common. The near-trench part or outer wedge, is often characterized by a series of active imbricate thrust faults, a subject of many observational, experimental, and theoretical studies (e.g., Mandal et al., 1997; Lohrmann et al., 2003; Gulick et al., 2004). The inner wedge, further landward, consists of older accreted sediments and margin rock framework exhibiting various transitions, from margin-parallel structures to those of

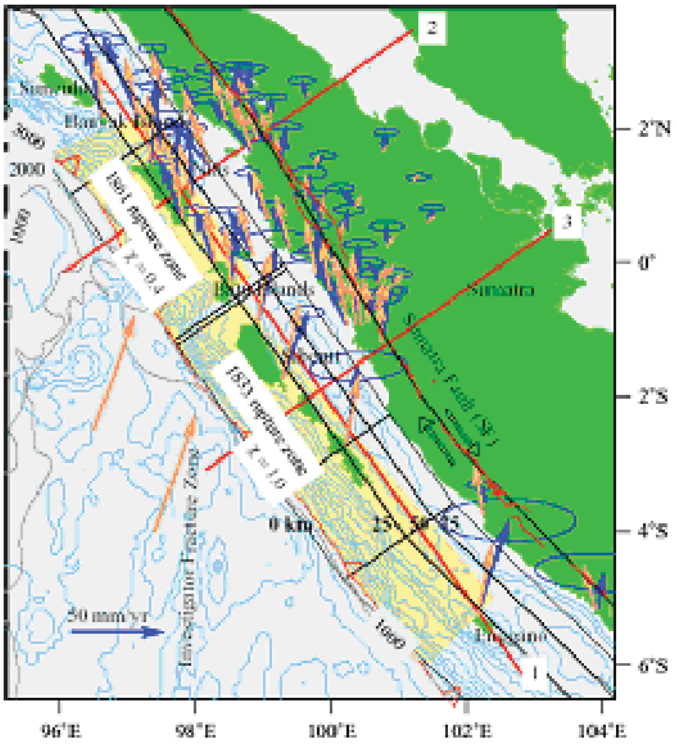

Figure 9. *Sumatra Observed GPS vectors (in blue) showing and modeled predictions (orange vectors) Rupture areas of the 1833 M 8.7 earthquake and the 1861 M 8.4 quake also shown. Northern poorly coupled indicated by nearly margin parallel GPS vectors. The 12/26 magnitude 9.0-9.3 event apparently ruptured from the north edge of the 1861 event to the northern end of the subduction zone. From Prawirodirdjo et al. 1997*

other orientations (if convergence is oblique), a break in slope, and in some cases a change in vergence (e.g., Cascadia; Goldfinger et al., 1992; 1997). Vergence flips may result from a thick sedimentary section and consequent overpressured sediments and low basal shear stress (low coefficient of friction) along the décollement, a seaward-dipping backstop, or basal section with contrasting physical properties (e.g., Seely, 1977; Byrne et al., 1993; Gutscher et al., 2001). Cascadia studies also indicate that complex vergence changes coincide with other structural indicators of reduced basal shear stress updip of the probable seismogenic zone (Goldfinger et al., 1992; 1996; 1997; Johnson et al, in press). The prism is a composite of many other elements also responsible for surface morphology: 1) strength boundaries that result from accretion and erosion events; 2) changes in incoming section thickness; 3) changes in décollement depth; 4) landsliding and normal faulting; and 5) duplex structures. These elements have only rarely been directly linked to physical properties of the prism and décollement and thus to the seismogenic zone, and drilling is the only technique for establishing such linkages. For example, offshore northern Sumatra, the toe of the prism is steep; the remaining prism forms a flat plateau (Fig. 4; Henstock et al., 2006, Ladage et al., 2006, Fisher et al., 2007). A postulated duplex structure imaged within this forearc (Fisher et al., 2007, Gaedicke et al., 2006) appears to influence outer arc high morphology, but we do not yet know how other factors have contributed, and what links exist to seismogenic rupture of this margin.

The position of the seismogenic zone relative to overlying wedge morphology is the subject of considerable debate. Compilations of past seismogenic rupture data suggest that moment release tends to underlie the inner wedge and outer forearc basin (Song and Simons, 2003; Wells et al., 2003 Bürgmann et al., 2005; Goldfinger and McNeill, 2006), but links to forearc rheology, history and structure remain poorly understood. Models of updip limits to seismogenic rupture vary considerably. Early models attempted to relate presence of forearc highs, basins, and intervening deformation zones directly to the mechanical consequences of “backstop” geometry. In these models, the forearc basin overlies the tip of the backstop, and thus is undeformed because it is “shielded” from interplate stress by the presence of the strong backstop (i.e., Byrne et al., 1993). Hyndman and Wang (1993) and Oleskevich et

al. (1999) later proposed updip and downdip limits to seismogenesis based primarily on thermal considerations (e.g. Scholz, 2003) moderated by dehydration reactions. Other authors debate the influence of temperature, hydrology and rheology/mineralogy on the plate boundary during earthquakes, where strain rate-dependent processes are significant and may control the extent of the seismogenic rupture (Saffer and Bekins, 2002; Moore and Saffer, 2001; Marone and Saffer, 2006; Moore and Lockner, 2006). Structure and geomorphology may indicate regions of coupling and potential seismogenic rupture. For example, changes in slope gradient and fault geometry (e.g., vergence) and orientation coincide on the Cascadia forearc at the inner-outer wedge transition, and are proposed as indicators of the updip seismogenic zone limit (Goldfinger et al., 1992; 1996; 1997). A similar inference for the updip limit has been made by Fisher et al. (2007) and Goldfinger and McNeill (2006) for Sumatra.

Classical Coulomb theory attempts to model accretionary wedges using time-averaged parameters over relatively long time scales (e.g., Lallemand et al., 1994), and commonly does not consider their composite nature, or the dynamics of earthquake rupture. Strong gradients in basal shear stress at the seismogenic limits may play a role in shaping observed wedge morphology. For example, Wang and Hu (2006) infer that the surface slope may be determined by peak basal stress during large earthquakes, not by interseismic processes. With all other factors equal, if a large earthquake causes the basal stress to rise to a very high level (i.e., velocity strengthening), the wedge will enter a compressively unstable regime, and must then deform in order to attain a greater slope angle, building greater surface slope over many earthquake cycles. This model may explain observed structural observations in wedges, where classical Coulomb theory cannot. However, the dynamic Coulomb model does not address the outermost wedge, seaward of the updip limit. Lateral compression near the toe has a backstop on both sides, since the incoming section on the subducting plate resists compression as well, so the resulting "pre-seismogenic" wedge may differ from the outer wedge farther landward. Wedge geometry may also be influenced by thickness changes in the incoming section. Outermost wedge faults may slip during great earthquakes, or soon after, and indeed must eventually slip since they are squeezed between the inner wedge and the incoming section. Whether these faults rupture seismically may be predictable with dynamic Coulomb theory. In either case, the outermost wedge may contribute to tsunamigenesis if it slips coseismically (Bilek and Lay, 2002) and has been suggested for the 2004 Sumatra event (Henstock et al., 2006; Grilli et al., 2005).

The evolution and resulting structure of the prism plays a critical role in its mechanical behavior and ultimately in rupture propagation. Available seismic observations of how slip propagates from the seismogenic zone seaward into an accretionary wedge reveal the contrasts in mechanical behavior that exist across many accretionary wedges. Our best observations include the Cascadia and Nankai, tsunamigenic wedges, to which we must compare Sumatra. Ruptures with significant moment are not believed to propagate readily through the seawardmost ~30 km of any prism, because incompetent, unconsolidated sediments and high fluid pressures cannot sustain sufficient shear stress (Moore and Saffer, 2001). Microseismicity, tsunami inversions, and estimates of physical properties from seismic observations, drilling and ancient analogues all suggest a transition from materials with velocity-weakening frictional properties in the landward or arcward portion of a margin (the inner wedge) to velocity-strengthening material in the seaward portion (the outer wedge) (Byrne

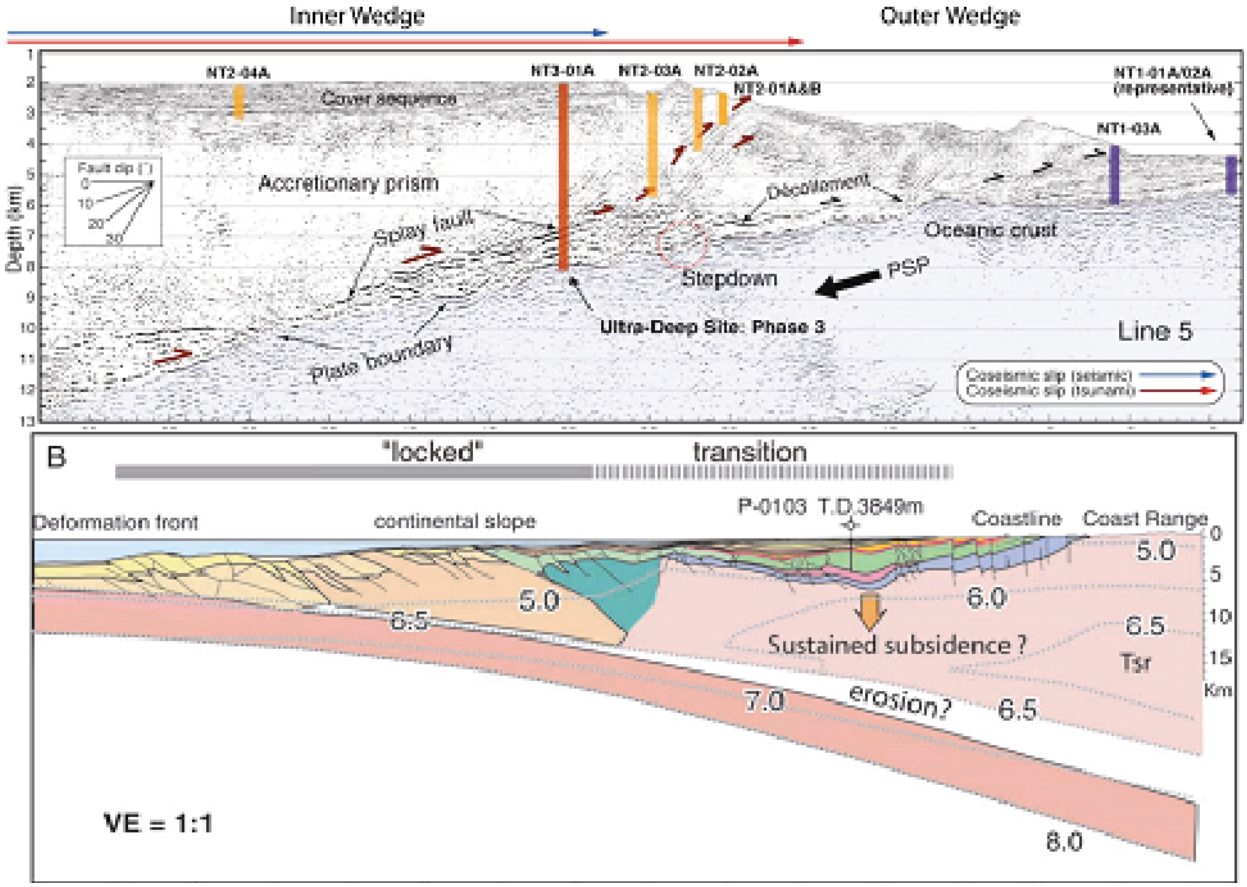

Figure 10. *Structure and geometry of two accretionary wedges. (A) Nankai, based on a seismic profile off the Kii Peninsula (Park et al., 2002). (B) Cascadia profile in central Oregon, modified from Wells et al., 2003). This proposal addresses linkages between major elements of the prism offshore Sumatra and seismogenesis -tsunamigenesis.*

et al., 1988; Marone and Scholz, 1988). An alternative model of rupture propagation proposes that slip may be directed through competent rocks of the inner wedge to the seafloor along an out of sequence thrust (OOST) or splay fault (Park et al., 2002) and altogether bypass the outer accretionary prism (**Figure 10**). Our current seismic (SCS and MCS) observations of Sumatra do not image such features, and Fisher et al. (2007) have suggested that shallow sediments are only weakly coupled with what they hypothesize to be a seaward–vergent duplexed plate boundary system at depth. Nonetheless, splay faults provide both a rupture pathway within the velocity weakening material and a more direct pathway to the surface than propagation of rupture to the trench. A broad understanding of prism architecture and evolution is critical both to the understanding of slip propagation through the prism and thus to seafloor displacement and tsunamigenesis: this can only be achieved with a combination of geophysics and drilling.

Mechanical properties that control rupture propagation through the outer accretionary wedge are also factors controlling deformational behavior producing the accretionary wedge architecture. Also linked to the prism evolution is thrust structure: vergence is thought to be an indication of the physical properties of sediments within the prism, within the incoming section and/or at the décollement. This suggests a link between seismogenic behavior of the plate boundary and overlying structure. Currently, it is unclear how prism structure is affected by or controls coseismic

plate boundary rupture (Wang and Hu, 2006), or how faults of differing geometry in the prism toe may behave during major plate boundary slip to produce possible surface rupture (e.g., Henstock et al., 2006). The predominant fault geometry within accretionary prisms is that of landward-dipping or seaward-vergent thrusts, forming an imbricate fold-thrust belt gradually growing seaward. Deviations from this simple geometry include OOSTs initiating and active within the older prism and seaward-dipping or landward-vergent thrusts developing in other parts of the prism. The latter style of faulting is relatively unusual in active accretionary prisms, with the main cited example the Cascadia margin from central Oregon to northern Washington (MacKay et al., 1995; Flueh et al., 1998; Goldfinger et al., 1996, 1997, Adam et al., 2004). Within the Cascadia prism, as ~ seven sequential thrust faults dip seaward (Adam et al., 2004); more commonly, only prism toe thrusts are affected, e.g., Gorda margin, (Gulick et al., 1998), Hellenic Trench, (Kopf et al., 2003) and Hikurangi margin, (Barnes et al., 2002).

Several models have been proposed for landward vergence, globally, summarized by Gutscher et al. (2001), including: a) low basal shear stress and high pore fluid pressure (Seely, 1997; Mackay et al., 1995 Goldfinger et al., 1997); b) an underlying ductile basal layer (Gutscher et al., 2001) and c) a seaward-dipping backstop (Byrne and Hibbard, 1987). The first mechanism is often related to thick, overpressured subducting sedimentary sections; for example, landward vergence in Cascadia coincides geographically with the subducting Astoria and Nitinat fans. While Adam at al. (2004) suggest that a limited duplex in calcareous sediments in Cascadia could play a role, the links and spatial correspondence with the fan sequences, and mud volcanoes on the abyssal plain, make it likely that overpressuring in the rapidly deposited and accreted fan section is responsible there.

The landward vergence shown in both seismic profiles and new multibeam mapping is consistent with the accretion of a large Pleistocene fan north of the equator. We infer that similar to the Washington margin, the rapid accretion of the Nicobar fan has probably resulted in high pore fluid pressures in the wedge, and low basal shear stress, as evidenced by the landward vergent, low tapering wedge (e.g. Seely 1977, McKay et al, 1992; Goldfinger et al., 1992; 1997). This may relate to the very slow rupture in the Andaman and Nicobar part of the rupture area. Further evidence of high pore fluid pressure in the northern forearc comes from mud volcanoes reported in the Andamans (Pal et al., 2003).

Continental Margin Morphology and Sedimentation

The morphologic details of the continental margin offshore Sumatra and the Andaman Nicobar region of the subduction zone have only been well imaged with swath bathymetry in a few locations prior to 2004 (Excepting naval data not in the public domain). The British hydrographic survey vessel HMS Scott has surveyed several significant portions of the margin in January and February 2005, and subsequent surveys by the German BGR, IFREMER, and JAMSTEC have competed multibeam survey of much of the Sumatra trench and outer forearc. (Henstock et al., 2006; Sumatra Aftershocks cruise report, 2006; Sonne SeaCause SO-186 cruise report, 2006). Figure 10 shows the deformation front at ~ 3^0 N. The asymmetry of the folds reflects the landward vergent frontal thrusts, also shown in seismic profiles in Karig et al., (1980; however Karig interpreted these as seaward vergent, despite the landward vergent asymmetric folds) and also visible are channel systems and numerous slide scars.

Three important issues that bear on the applicability of turbidite paleoseismology to the Sumatran margin are 1) the presence of channel systems to deliver seismically triggered turbidites 2) the presence of planktonic Forams for radiocarbon dating, and 3) the favorability of physiography for limiting turbidites from other sources.

Channel Systems: The new data from HMS Scott, BGR and IFREMER show that well developed channel systems do exist, though the full pathways and headwaters are in some cases not known (**Figure 11**). Most channel systems appear to head in the outer arc ridge, and do not penetrate the forearc plateau to a great degree or reach the forearc basin. On the seaward flanks of the major forearc islands of Simeulue, Nias, Siberut, Pagai, Sipora and Enganno, we observe multiple channels leading seaward down the continental slope and piggyback basins in their path. Due to the likely non-earthquake sedimentation events sourced in shallow water, we tended to avoid sites affected by these channels. In our Cascadia and SAF work, we have found that the active sediment source is not particularly important, nor is a contemporary terrestrial source even needed to produce a good turbidite record of seismic events. Several channels along the northern California margin have been displaced far from their

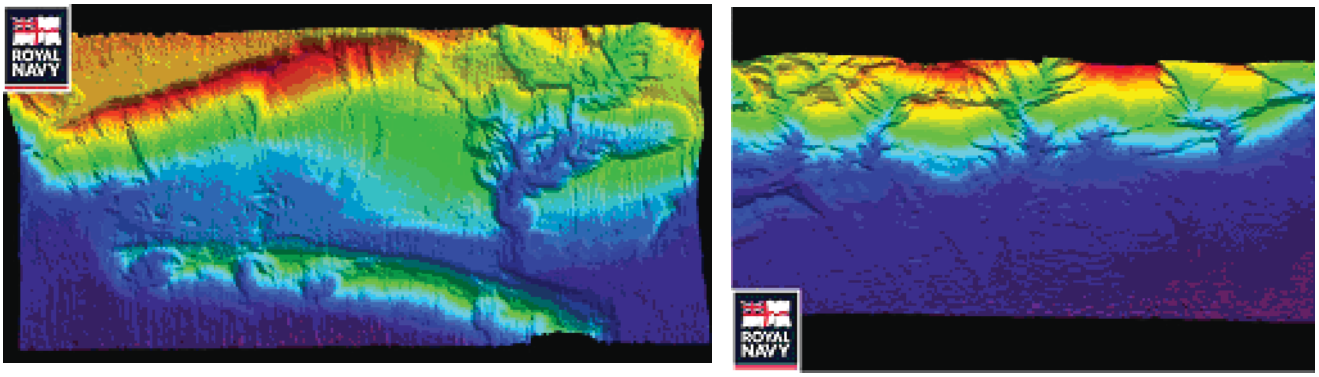

Figure 11. *Left: Deformation from at ~3^0 N, showing landward vergent folds, and slope/abyssal plan channel systems. Right: Five channels systems feeding the abyssal plain between mainland northern Sumatra and Simeuleu Island. We intend to focus on these deeper systems, with selected cores in forearc basin sites. Images courtesy of the British Geological Survey/Royal Navy/Southhampton Oceanography Centre Team & the United Kingdom Hydrographic Office..*

original sources, and have no modern source of sediment. These channels contained the same turbidite record as those that have sources, showing that with enough shaking, material along the canyon walls will fail, generating turbidity currents without a modern sediment supply (Goldfinger et al. 2007)

Foram abundance: The regional CCD is at ~4500-5100 m depth at these low latitudes (Tucker and Wright, 1990; Shulte and Bard, 2003). The Sunda trench deepens southward from ~ 3000 m to ~4500 m at the southern limit of the 2004 rupture, and should be above the CCD from 2^0 S to 14^0 N. On the Nicobar fan, Bandopadhyay and Bandyopadhyay (1999) report that pelagic sedimentation in the Holocene section is a foram ooze, and overlies an older unit aged ~ 8000 years consisting of fan turbidites, except for a narrow ribbon of turbidites present in the base of slope channel. The abrupt shift from fan turbidite deposition to pelagic foram ooze at ~ 8000 years is consistent with reports of blockage of the trench from northern sediment sources in late Pleistocene earliest Holocene time. Other core data are somewhat sparse from

the Sunda trench area, however we find about 50 cores in the general area in the NGDC database, 15 of these are in a database of core-top foram assemblages (Prell et al., 1999). Several of these cores are in the trench between 2^0S and 15^0N. The high foram abundances from the near surface sediments reported in the core-top database indicate that abundance is more than adequate for radiocarbon dating. *G. Menardii* abundance is also high, and these large individuals improve dating precision by reducing the sediment thickness needed for each ^{14}C age.

Margin Physiography: A key feature that made Cascadia Basin a good paleoseismic recorder proved to be the relatively wide continental shelf of Oregon and Washington (Goldfinger et al., 2003b; 2004; submitted). Under high-stand conditions, the shelf separates rivers from their associated canyons, which are completely infilled by transgressional sediments. This configuration apparently prevents hyperpycnal flows from connecting to canyon systems and generating turbidity currents (Sternberg, 1986). In Sumatra, the separation is even greater, with a wide forearc basin and forearc high separating land sources from lower slope and abyssal plain channels. While complete bathymetric data do not yet exist, we believe that land derived flows directly into the trench are highly unlikely because of this separation, and the apparent blockage of the trench from northern (Himalayan sourced) sediment input.

Coring Approach

This project seeks to apply the turbidite paleoseismologic techniques that have been successful in Cascadia to the mainshock region of the 2004 Sumatran earthquake. We propose a cruise to collect a suite of cores along the Sunda trench to address the long term earthquake record from the mainshock region and adjacent segments along the Sumatran subduction zone. The lack of this type of information certainly has contributed to the unprecedented disaster of December 26th. That the rupture occurred in a region of mostly strike-strike slip interaction, and apparent poor coupling, is puzzling. Does the apparently low coupling mean a very long recurrence interval? Or have we underestimated the convergence due to poor GPS coverage and poorly known rates of Andaman Sea opening? In any case, the earthquake history of this subduction zone is of great scientific and societal interest, and we believe it can be determined from the turbidite record. Unlike Cascadia, where marsh paleoseismology was needed to establish that there *was* a great earthquake record, this is already known in Sumatra. Of further interest, the calibration of the turbidites deposited during the recent earthquake will be of use in calibrating the seismic history of Sumatra, but also of Cascadia, which has many parallels to the Sumatran system. For example, will we see the subevents in the 2004 turbidite? Did the slow northern rupture trigger turbidity currents? Might this be like the Washington Margin with its low taper and accreting fans? Sumatra has a relatively short record of historically recorded earthquakes, but has a high precision record of paleoseismology on land,

though of shorter duration. Combined, the land and marine records should, as in Cascadia, provide a Holocene earthquake record complete to ~ the M8 level.

This project has three principal objectives:

- To collect a sufficient number of new cores to sample the mainshock and adjacent segments of the Sumatran margin in the Sunda trench, and establish the turbidite event history with AMS ^{14}C, hemipelagic thickness and correlation techniques.

- To test the event record using both synchronous triggering criteria between sites, and sedimentological origin to test for earthquake origin.

- To test for segmented and multiple segment ruptures using radiocarbon and physical property correlations, and establish the long term frequency and pattern of earthquakes in the Holocene.

Do the Sumatran turbidites represent subduction earthquakes exclusively (**Figure 12**)? During the analysis phase, we will apply the methods for synchronous testing we have used in Cascadia and the San Andreas, and also use sedimentological criteria developed by Japanese investigators as described in the preceding sections (e.g. Nakajima and Kanai, 2000).

Can Adams' and our triggering arguments be applied to Sumatra? Clearly some of them cannot, as we already know that the margin is segmented, and thus synchroneity along the entire margin is not the case. It is conceivable that historically unknown large earthquakes trigger all segments, and if so the turbidite record will strongly favor these larger events. Arguments against storm and distal tsunami triggers are applicable to other margins, and all margins may have a component of noise from small crustal and intraslab earthquakes. On the Sumatran margin, discreet drainage systems exist but are poorly known, and a relatively modest sediment supply is delivered from the shelf to the trench. Therefore, oversteepened slopes due to high sedimentation rates seem an unlikely trigger in this region, particularly in light of the frequent seismic triggers. Cascadia, with high sedimentation rates and less frequent (~600 yrs) triggers, seems little affected by this process. Thus, earthquakes appear to be the best turbidite triggers for Sumatra as well. Possible triggering of turbidites by typhoons in Sumatra is a factor not present in Cascadia. Typhoons can bring both high sediment flux and large significant wave heights. Large storms might trigger turbidity currents by hyperpycnal flow if the physiography is favorable (Mulder and Syvitsky, 1995), or by loading from large storm waves. In Sumatra, the forearc basin appears to trap sediment from the mainland and from the eastern coasts of the offshore islands. Thus direct high flux to canyon heads is unlikely. Storm wave loading from typhoons is similar to that of large extra-tropical cyclones such as those in Cascadia. Maximum significant wave heights for both are similar at 20-25m, with the highest single wave ever recorded being 34 m in a hurricane. We have found no evidence for storm deposits on the abyssal plain in Cascadia (except in the Eel basin as noted above), and infer that such deposits are even less likely in Sumatra due to the intervening unfilled forearc basin.

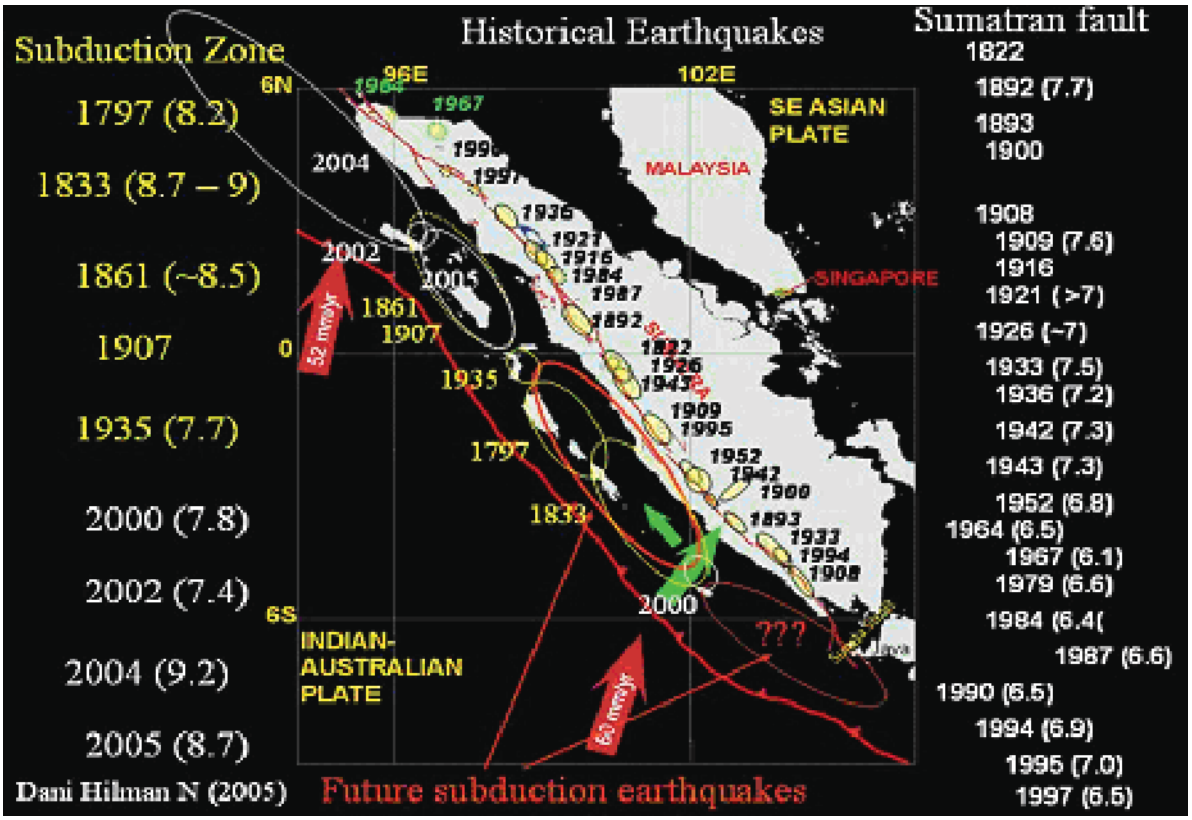

Figure12. Compilation of historical and paleoseismic data for past Sumatran earthquakes showing segmentation of the subduction interface possibly detectable in the turbidite record.

Cruise Synopsis

The cruise was staged from Phuket Thailand, and both departed and returned to that port. The strategy was to core trench sites on the southbound leg, and to core basin sites on the outer arc high on the return, in addition to repeating some sites. The average spacing of sites along the margin was ~ 80 km, close enough to identify seismic segments and obtain cores on areas that may show overlap of turbidity currents triggered in adjacent seismic segments. Using existing and newly collected multibeam and sub-bottom records, core sites were chosen along the Sunda trench and slope basins. After cores were collected, all were analyzed using the OSU Geotech MST system, collecting gamma density, p-wave velocity, resistivity high resolution imagery and point and loop magnetic susceptibility series for each core. Cores were then split and hand logged at sea, and imaged with the Geotek high-resolution line-scan camera system.

Core Siting

Core siting was made using multibeam bathymetric data from the EM-120 system, associated backscatter and sidescan data, and sub-bottom profiling. Bathymetric data was graciously supplied from the UK, French, Japanese, and German investigators working in the region and greatly aided our ability to focus on site selection strategies without the need to map new unmapped areas. In some cases we remapped selected areas where existing data were of poor quality. We also employed Parasound sub-bottom profiles supplied by the BGR (Germany) which

greatly improved our ability to interpret meso-scale sedimentary and tectonic features using deeper penetration than available on the Revelle 3.5 kHz chirp subbottom profiler. We collected continuous 3.5 kHz chirp profiles along the ship track, and conducted numerous site surveys to evaluate the stratgraphy of potential core sites and compare previous cores to their associated sub-bottom records.

A key feature that made Cascadia Basin a good paleoseismic recorder proved to be the relatively wide continental shelf of Oregon and Washington (Goldfinger et al., 2003b; 2004; submitted). Under high-stand conditions, the shelf separates rivers from their associated canyons, which are completely infilled by transgressional sediments. This configuration apparently prevents hyperpycnal flows from connecting to canyon systems and generating turbidity currents (Sternberg, 1986). In Sumatra, the separation is even greater, with a wide forearc basin and forearc high separating land sources from lower slope and abyssal plain channels. While complete bathymetric data do not yet exist, we believe that land derived flows directly into the trench are highly unlikely because of this separation, and the apparent blockage of the trench from northern (Himalayan sourced) sediment input.

Sites were generally selected with channel systems leading from the accretionary wedge as the focus. While some earthquake generated turbidites likely exist in the main forearc basin of Sumatra and its sub-basins, these are almost certainly mixed with land-derived storm and flood deposits from the Sumatran mainland, thus making the turbidite record much more complex. We chose to use the trench and outer forarc basins for the focus on paleoseismology to simplify the source mechaninsms by eliminating land-derived events from the record.

Small channels generally formed small fans or aprons on the trench floor. Many were surrounded by annular bedforms with a single active central channel leading away from the margin. Because the age of the Indian Plate generally increases southward, the regional slope of the Sunda trench is to the south. Channels generally flow southwestward into the trench and curve to the south into the trench axis. In the northern part of the survey area, the Nicobar Fan sediments fill the trench, with a thicknesss of ~ 3 km. This trench fill thins southward, and basement structure is more apparent southward along the Sunda Trench. The investigator Fracture Zone, the Wharton Ridge, and several other fracture zones segment the trench into sediment basins (and likely into seismic segments as well). The central to southern part of the Sunda outer trench wall is characterized by numerous trench parallel normal faults dipping both east and west forming graben valleys. These grabens have captured old channel systems and capture margin derived turbidites as well as generating mass wasting deposits of their own that fill the grabens.

Our site strategy was to seek margin turbidites while avoiding turbidites possibly shed from other sources such as the subducting fracture zones and ridges, basement normal faults, and Indian Plate seamounts. We preferred sites that were protected from turbidity currents sources from the west and used west facing normal faults to capture possible western sourced events and prevent them from reaching the trench floor. We also preferred landward vergent segments of the lower slope thrust systems as these proved to be reliably less sandy areas due to the greater dissection and sand supply shedding from the seaward vergent regions. Detailed site selection was made by comparing past cores with the sub-bottom record to fine tune the amount and grain size of the turbidites by either moving to sites more or less proximal from the local sand sources.

Age Control

We will apply dating techniques as we have in Cascadia to directly date planktonic forams either just above or just below the turbidites. In some cases we may use samples from above and below the turbidite tails where we suspect erosion. Abundance of planktonic forams in these water depths is adequate though the hemipelagic sedimentation rate in the trench is not known at present. We need a minimum of approximately 400 individuals depending on species and size for each AMS date to reach the 2 mg minimum sample weight requirement. The regional CCD is at ~4500-5100 m depth at these low latitudes (Tucker and Wright, 1990; Shulte and Bard, 2003). The Sunda trench deepens southward from ~ 3000 m to ~4500 m at the southern limit of the 2004 rupture, and should be above the CCD from 2^0 S to 14^0 N. On the Nicobar fan, Bandopadhyay and Bandyopadhyay (1999) report that pelagic sedimentation in the Holocene section is a foram ooze, and overlies an older unit aged ~ 8000 years consisting of fan turbidites, except for a narrow ribbon of turbidites present in the base of slope channel. The abrupt shift from fan turbidite deposition to pelagic foram ooze at ~ 8000 years is consistent with reports of blockage of the trench from northern sediment sources in late Pleistocene earliest Holocene time. Other core data are somewhat sparse from the Sunda trench area, however we find about 50 cores in the general area in the NGDC database, 15 of these are in a database of core-top foram assemblages (Prell et al., 1999). Several of these cores are in the trench between 2^0S and 15^0N. The high foram abundances from the near surface sediments reported in the core-top database indicate that abundance is more than adequate for radiocarbon dating. *G. Menardii* abundance is also high, and these large individuals improve dating precision by reducing the sediment thickness needed for each ^{14}C age.

We used a 4” diameter piston corer with a 4” diameter trigger corer. We also deployed our 20cm square Jumbo Kasten corer, built specifically for paleoseismic work on the San Andreas Fault. This 3m corer is designed to minimize core disturbance, while maximizing sample volume in the upper 3m of section (i.e. Skinner and McCave, 2003). Age control post-cruise also will be derived from correlation with paleomagnetic secular variation curves for the region, described below. In Cascadia we have not found bioturbation to be a significant issue, but this may be the result of high sedimentation rates. If low rates are encountered in hemipelagic sediments of the Sunda trench we will explore corrections for bioturbation such as outlined in Horng et al. (2002) and references therein. Following the cruise, AMS ages will be determined from planktonic forams. Forams will be sieved @63m, and washed at A. Mix’s paleoceanographic laboratory at OSU. This group is highly experienced in processing and identification of late Quaternary microfossils. The forams will be picked and identified to species level by an experienced oil industry consultant we have used for 5 years. AMS ages will be determined at the Woods Hole Accelerator Mass Spectrometry facility. Raw AMS ages will be reservoir corrected and converted to calendar years by the method of Stuvier and Braziunas (1993) using reservoir values for the Indian Ocean (Southon et al., 2003; Hua et al, 2004). Our Cascadia reservoir corrections have replicated the known ages of the 1700 Cascadia earthquake and Mazama eruption within 10 and 40 years respectively, however some sites show significant reservoir excursions. These apparent excursions are now being investigated in a separate project. The application of AMS dating to marine microfossils is an

evolving field-tied advances in paleoceanography. We will keep abreast of ongoing work in order to apply the most recent findings to the 14C calibration of our samples.

Physical Property Correlation

At sea we acquired point and loop magnetic susceptibility, Gamma density, P-wave velocity, resistivity and high resolution line scan imagery with our Geotek MST system and separate high-resolution point-magnetic track system as we have done in Cascadia and SAF work. We collected all data at 0.5 cm sample interval. Magnetic susceptibility and gamma density have proven invaluable for event correlation as discussed above. We will augment these measurements with X-radiography post-cruise. In order to further improve our ability to correlate events in the cores, we will also employ U-channel technique as a pilot study to add paleomagnetic secular variation to the suite of correlation tools available. U-channel paleomagnetic measurements can provide a way of facilitating correlation of sediment sequence through reconstruction of past changes of the geomagnetic field and through the development of tracers of lithologic variability that go beyond what can be done using an MST track alone (Stoner et al., 1996; Stoner and Andrews 1999). The U-channel samples are collected by pushing rigid u-shaped plastic liners (2 x 2 cm cross-section) that are up to 1.5 m in length, into the split halves of core sections. The u-channel sample comes from the pristine center part of the core, minimizing disturbance, and therefore improving not only magnetic but also physical properties measurements. Measurements are made at 0.5 cm intervals and through deconvolution (i.e., Guyodo et al., 2002) the ~4.5 cm of stratigraphic smoothing (Weeks et al., 1993) can be significantly reduced. The resultant paleomagnetic, rock magnetic and physical properties data can be used to develop directional paleomagnetic secular variation (PSV) and relative paleointensity (RPI) curves as well as records of environmental variability. Systematic century to millennial changes in the Earth's magnetic field when properly recorded in sediments provide chronostratigraphic templates that can be use for regional (PSV) (e.g., Thompson 1984; Lund 1996; Stoner et al., 2004) and to global (RPI) correlations (Stoner et al., 2000; Laj et al., 2004). PSV has a long history in lake sediment studies (e.g., Thompson 1973; Thompson and Turner, 1979, Verosub et al., 1986; Lund 1996; Brachfeld and Banerjee, 2000; Ojala and Tiljander, 2003) and recent work on marine sediments demonstrate (Lund and Schwartz 1996; Kotilainen et al., 2000; Verosub et al., 2001; St-Onge et al., 2003) that PSV can provide a viable means of marine/marine and marine/terrestrial correlation at resolutions equivalent to, and in some case better than, what can be achieved through radiocarbon dating (Lund 1996; Hagstrum and Champion, 2002; Stoner et al., 2004; Stoner et al., in prep). Hagstrum et al., (2004) and St-Onge et al., (2004) have now demonstrated that PSV is applicable to paleoseismic studies.

Newly acquired and unpublished data from Steve Lund (**Figure 13**) show that the Indonesian region is characterized by well-resolved centennial to millennial scale PSV. Spherical harmonic global field models (Korte and Constable 2005) suggest that this applies to the RPI records as well and show that Lund's data from eastern Indonesia would be valid as an initial dating curves for the Sumatra region. Therefore, applicable PSV templates are already available. New observations from the Indonesian region would further refine our understanding space/time geomagnetic patterns and the continued development global scale paleo-geomagnetic field model (e.g., Korte

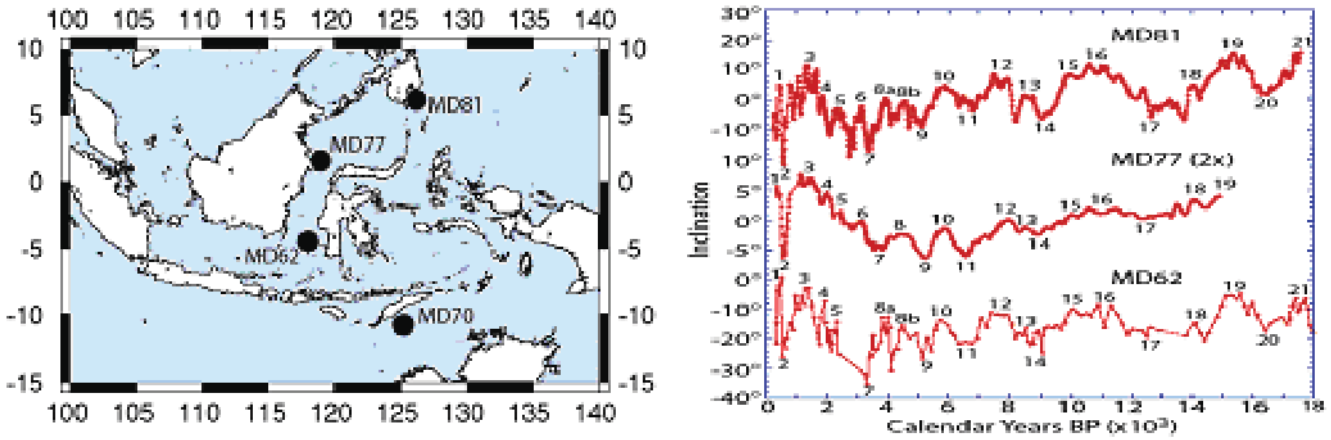

Figure 13. A: *Location map of three paleomagnetic cores shown in B. B. Paleomagnetic inclination plot for the three cores at left. Good correlation during the Holocene and latest Pleistocene is apparent in the region, indicated by the correlative numbers above each plot (1-21). The PSV signature adds a third timeline to the chronostratigraphic framework for Indonesian cores. Courtesy of S. Lund.*

and Constable 2005). Such information will be vital for assessing spatial scales of newly documented high frequency geomagnetic field behavior (e.g., Gallet et al. 2003) and the long term role of the geomagnetic field in shielding the Earth from cosmic rays and the production of cosmogenic isotopes (St-Onge et al., 2003; Hughen et al., 2004). Correlations between cosmogenic isotope records and climate records (e.g., Bond et al., 2001; Hodell et al. 2001) make this of fundamental importance.

Ash Stratigraphy

Ash-bearing turbidites are common in the Holocene Sumatra trench fill (e.g. Martin-Barajas, A. and Lallier-Vergas, 1993). The Toba Ash, erupted from the Toba Caldera, Sumatra, is a major stratigraphic marker in the Indian Ocean that is correlable in deep sea cores from the Bay of Bengal (Pattan et al., 2002). Major, trace and REE composition and morphology of the shards suggest Youngest Toba Tuff (YTT) of 74 ka. The detailed trace element concentration ratios (La/Lu, Zr/Hf, Nb/Ta, Zr/Nb, Cs/Yb, Ce/Y and Rb/Sr), major elements, REE composition, chondrite-normalized REE pattern and bubble wall junction-type morphology of glass shards from the CIOB match well with proximal sample from Northern Sumatra (Toba caldera; Pattan et al., 2002) Examples of the YTT reported from Bay of Bengal, India, Malaysia, ODP site 758, Arabian Sea and South China Sea (Pattan et al, 2002 and references therein). The Toba eruptions dated ~ 74,000 years BP, ~ 540,000 years BP and ~ 840,000 years BP, are known as the Youngest Toba Tuff (YTT), Middle Toba Tuff (MTT) and Oldest Toba Tuff (OTT) respectively (Chesner, 1988). The YTT eruption from the Toba caldera was the earth's largest Quaternary volcanic event, covering nearly 1% of the earth's surface. Other datable and correlable ashes in the Sunda Trench were found in the cores that we expect will strengthen the stratigraphic framework.

Summary of Results

This project could not have been done without close collaboration with colleagues at NOC,S, IFREMER, and BGR who provided critical bathymetric and sub-bottom profile data. These data allowed our project to proceed directly to site selection, with very little bathymetric survey required. We typically required only

1-3 hours of 3.5 kHz sub-bottom profiling to select sites that had the needed section thickness and density for coring, basing on proximal/distal relationships to the local sediment sources.

Lithology and Sediment Sourcing

The primary sediment, ubiquitous along the Sumatran trench, is fine, well-sorted, mature biotite-rich quartz sand from a Himalayan source. These clean sands contained little else but occasional ash glass shards and radiolarians. These sands have been accreted, remobilized and deposited as turbidites in the trench floor and adjacent outer trench wall and slope basins. These sands were originally part of the Nicobar fan, a now inactive lobe of the eastern Bengal fan that may have been isolated by impingement of the Ninety-East Ridge on the Sunda Trench at ~ 09N (Curray, in press). Whether the trench south of this point is in fact isolated from Himalayan sources turbidity currents is not completely certain however, and no modern multibeam surveys exist to test this hypothesis. These fine sands off Sumatra are sources up to 2700 km from their site of deposition, accounting for their maturity. Hemipelagic sediment is rare in the trench axis, suggesting either a very slow sedimentation rate, or very frequent turbidity current occurrence. Ashes were found sporadically in trench cores. All cores had prominent diagentic fronts at 5-25 cm from the core tops, above which were oxidized units near the seafloor surface. These fronts appear to be an upward migrating diagenetic reaction that roughly keeps pace with the local sedimentation rates. The trench cores were for the most part barren of calcareous microfossils excepting rare examples buried in turbidite tails. In sites adjacent to forearc islands, some cores recovered turbidites with elevated organic content that was apparent visually, and most likely resulted from local input from the islands. Cores located between forearc islands did not include such organic rich intervals. The mean grain size generally decreased southward along the margin, consistent with the original southward sediment transport along the Nicobar Fan prior to accretion to the margin and subsequent uplift. Magnetic susceptibility records remained consistently low along the margin despite the grain size decrease, most likely because the magnetic particles were in the silt, not the sand size fraction as is observed elsewhere (Goldfinger et al., 2007).

Sources for sampled turbidites most likely are local slope sources. In many cases, channel systems leading directly from the margin were observed and sampled. In cases where the local source was not apparent from the channel/apron morphology, the thickness and reflectance in sub-bottom profiles decreased away from observed accretionary wedge source features such as dissected canyons, failed fold limbs, and outlets from frontal thrusts that plunged or terminated. We saw little evidence of local trench parallel transport, and indeed the bathymetric gradients were typically ~0.05 degrees, offering little gravitational incentive for trench parallel transport. Azimuths for channel systems exiting the accretionary wedge ranged from 10 degrees upstream of trench normal to ~ 15 degrees downstream, showing a slight preference for transport down the trench axis, but local constructional slopes on fan surfaces commonly dictated local flow direction. Several major channel systems observed on the BGR multibeam data seaward of the trench axis trended away from the trench axis, disappearing to the west at the coverage limit. The channels however were not useful for paleoseismic sampling as they were found to be involved with the most recent episode of basement bending moment normal faults, and segmented into isolated

relict segments. The trench itself is compartmented by the Investigator fracture zone, the Wharton Ridge, and other unnamed fracture zones, further inhibiting trench parallel transport.

Locally, secondary turbidite sources were observed at basement normal fault and basement seamount localities as sand aprons thinning away from these locations. These secondary sources were avoided as much as possible during site selection. In sites near potential secondary sources, we observed no elevated mafic content or increased magnetic susceptibility that would be expected from local basement basaltic sources, and conclude that at least in our onboard preliminary analysis that input from these sources was negligible.

In examination of calcareous microfossil assemblages, we found good preservation above about 3500m water depth, and significant erosion of tests at greater than 4100m, suggesting the CCD lies between these depths, shallower than previously reported. In slope basin sites above the Holocene CCD foram sands dominate the record, with tubidites secondary, and ash layers somewhat more common than in the trench. In order to develop a strategy for dating the tubidites, we chose to obtain slope basin records above the CCD that could be correlated along strike, and with the trench cores to establish a temporal and stratigraphic event framework. Foram abundance was so great at shallow sites above 2000m that we adjusted our site selections for optimal section thickness by targeting sites ~ 3500 m for good foram preservation without overwhelming the record with foram sand as we found in several cores at shallower sites. Deeper sites had less than optimal preservation.

Local slope morphology played a key role in the local sand supply on the trench axis and near axis sites. The overall morphology of the continental slope, as previously noted, comprises a broad terrace off the north part of Sumatra, tapering to a narrower forearc high in the south. The drainage and erosion pattern of the outer slope is an unusually dissected form, particularly considering the absence of througoing channel systems from the Sumatra mainland. While there are several large channel systems sourced on the western shelves of the larger islands such as Nias, and Siberut, most of the erosion is local and related to failure and headward erosion in individual basin systems. This erosion is much more extensive than observed in Cascadia, Nankai and most other acretionary prisms. We found in our sampling, that at sites in the trench axis opposite heavily eroded margin segments, the sand content was consistently greater. These areas in turn were strongly linked to thrust vergence, with the lower dips of landward vergent areas less prone to failure and erosion. We infer that the highly dissected morphology of the outer slope is the result of the mature fine sand composition of the fold thrust belt, which we sampled in the trench turbidites. The highly mature quartz sand has little cohesion, and the hemipelagic sedimentation rate is low, thus much of the slope is likely composed of these mature and easily eroded Nicobar fan sands.

Site Information

Core site maps are located in **Appendix 2** and **Appendix 3**. Plan view maps in three scales have sites plotted in **Appendix 2**. 3.5 kHz sub-bottom profiles are shown for all sites where data were collected. Oblique views of sites are shown in **Appendix 3**. Below is a summary of core sites including type of core, date of collection, core coordinates, water depth at core site, and length of recovered sediment (**Table 2**).

Table 2. Core Sites for Paleoquakes07.

Site #	Core #	Type	Date (GMT)	Latitude dd	Longitude dd	Depth (m)	Length (m)
1	RR0705-01GC	Gravity	5/7/03	4.566	92.969	4434	0.18
2	RR0705-02GC	Gravity	5/8/03	4.537	92.934	4483	0.00
2	RR0705-03TC	Trigger	5/8/03	4.537	92.934	4483	1.91
2	RR0705-03PC	Piston	5/8/03	4.537	92.934	4483	2.73
3	RR0705-04KC	Kasten	5/8/03	4.307	92.934	4540	0.00
4	RR0705-05TC	Trigger	5/9/03	4.480	92.927	4498	0.91
4	RR0705-05PC	Piston	5/9/03	4.480	92.927	4498	3.08
4	RR0705-06KC	Kasten	5/9/03	4.480	92.927	4498	0.00
4	RR0705-07MC	Multi-core	5/10/03	4.480	92.927	4498	0.00
5	RR0705-08GC	Gravity (BB)	5/10/03	3.605	93.318	4502	0.00
9	RR0705-14GC	Gravity	5/12/03	3.569	93.496	4414	0.00
6	RR0705-09GC	Gravity	5/11/03	3.570	93.130	4541	0.00
7	RR0705-10GC	Gravity	5/11/03	3.457	93.025	4481	0.23
8	RR0705-11GC	Gravity (BB)	5/11/03	3.482	93.065	4515	0.00
8	RR0705-12GC	Gravity (BB)	5/11/03	3.482	93.065	4516	0.55
8	RR0705-13KC	Kasten	5/12/03	3.482	93.065	4523	0.00
10	RR0705-15GC	Gravity	5/12/03	3.287	94.035	1912	0.34
10	RR0705-16GC	Gravity (BB)	5/12/03	3.287	94.035	1911	1.95
10	RR0705-17KC	Kasten	5/12/03	3.287	94.035	1911	0.00

Site #	Core #	Type	Date (GMT)	Latitude dd	Longi-tude dd	Depth (m)	Length (m)
11	RR0705-18GC	Gravity (BB)	5/13/03	3.276	94.020	1820	3.14
11	RR0705-100MC	Multi	6/8/03	3.276	94.020	1819	0.03
11	RR0705-101GC	Gravity	6/8/03	3.276	94.020	1823	0.53
12	RR0705-19GC	Gravity	5/13/03	2.248	94.514	4816	0.68
12	RR0705-20GC	Gravity (BB)	5/13/03	2.248	94.514	4816	2.21
13	RR0705-21GC	Gravity	5/13/03	2.273	94.539	4834	0.40
14	RR0705-22GC	Gravity	5/14/03	1.636	95.568	4985	0.94
14	RR0705-23GC	Gravity (BB)	5/14/03	1.636	95.568	4973	2.09
15	RR0705-24GC	Gravity	5/14/03	1.636	95.568	4975	0.99
16	RR0705-25GC	Gravity	5/15/03	1.067	96.467	5224	0.00
17	RR0705-26GC	Gravity	5/15/03	0.995	96.372	5220	0.45
17	RR0705-27GC	Gravity (BB)	5/15/03	0.995	96.372	5214	2.32
17	RR0705-87TC	Trigger	6/4/03	0.995	96.372	5211	0.77
17	RR0705-87PC	Piston	6/4/03	0.995	96.372	5211	5.02
18	RR0705-28GC	Gravity (BB)	5/15/03	0.080	97.045	5238	0.00
19	RR0705-29GC	Gravity	5/16/03	0.008	97.008	5303	1.39
19	RR0705-30GC	Gravity (BB)	5/16/03	0.008	97.008	5303	1.70
19	RR0705-84TC	Trigger	6/3/03	0.002	96.993	5305	1.11
19	RR0705-84PC	Piston	6/3/03	0.002	96.993	5305	3.44
20	RR0705-31GC	Gravity	5/16/03	-0.859	97.430	5420	1.37

Site #	Core #	Type	Date (GMT)	Latitude dd	Longi-tude dd	Depth (m)	Length (m)
21	RR0705-32GC	Gravity (BB)	5/16/03	-0.859	97.442	5435	1.83
22	RR0705-33GC	Gravity	5/17/03	-1.283	97.678	5489	0.00
23	RR0705-34GC	Gravity	5/17/03	-1.288	97.663	5463	0.81
24	RR0705-35GC	Gravity (BB)	5/17/03	-1.288	97.650	5455	1.99
24	RR0705-36KC	Kasten	5/17/03	-1.288	97.650	5455	1.85
24	RR0705-78TC	Trigger	6/1/03	-1.288	97.650	5455	1.52
24	RR0705-78PC	Piston	6/1/03	-1.288	97.650	5455	4.44
25	RR0705-37GC	Gravity	5/18/03	-1.707	97.921	5492	0.88
26	RR0705-38GC	Gravity (BB)	5/18/03	-1.699	97.938	5511	1.87
26	RR0705-39KC	Kasten	5/18/03	-1.699	97.938	5510	2.30
27	RR0705-40GC	Gravity	5/18/03	-2.134	98.221	5529	1.22
28	RR0705-41GC	Gravity (BB)	5/19/03	-2.129	98.244	5540	1.62
30	RR0705-43GC	Gravity	5/21/03	-2.232	98.356	5555	0.84
30	RR0705-44MC	Multi-core	5/21/03	-2.232	98.356	5557	0.00
30	RR0705-45TC	Trigger	5/21/03	-2.232	98.356	5561	1.37
30	RR0705-45PC	Piston	5/21/03	-2.232	98.356	5561	4.70
29	RR0705-42GC	Gravity	5/21/03	-2.016	98.773	1152	0.16
31	RR0705-46GC	Gravity	5/22/03	-2.942	98.868	5813	1.47
31	RR0705-47TC	Trigger	5/22/03	-2.942	98.868	5726	1.51
31	RR0705-47PC	Piston	5/22/03	-2.942	98.868	5726	2.72

Site #	Core #	Type	Date (GMT)	Latitude dd	Longi-tude dd	Depth (m)	Length (m)
32	RR0705-48GC	Gravity	5/22/03	-3.268	99.275	5790	1.70
32	RR0705-49TC	Trigger	5/23/03	-3.268	99.275	5797	2.58
32	RR0705-49PC	Piston	5/23/03	-3.268	99.275	5797	3.97
33	RR0705-50GC	Gravity	5/23/03	-3.658	99.604	5806	1.07
33	RR0705-70TC	Trigger	5/30/03	-3.658	99.604	5804	1.81
33	RR0705-70PC	Piston	5/30/03	-3.658	99.604	5804	5.09
34	RR0705-51GC	Gravity	5/23/03	-4.148	99.953	5987	0.00
35	RR0705-52GC	Gravity	5/24/03	-4.313	100.097	5991	0.14
36	RR0705-53GC	Gravity	5/24/03	-4.591	100.257	6063	0.17
36	RR0705-54GC	Gravity	5/24/03	-4.591	100.257	6061	0.43
37	RR0705-55TC	Trigger	5/24/03	-4.520	100.213	6046	0.00
37	RR0705-55PC	Piston	5/24/03	-4.520	100.213	6046	2.61
38	RR0705-56GC	Gravity	5/25/03	-5.440	100.799	6069	0.00
38	RR0705-57TC	Trigger	5/25/03	-5.440	100.799	6069	0.00
38	RR0705-57PC	Piston	5/25/03	-5.440	100.799	6069	4.86
39	RR0705-58GC	Gravity	5/25/03	-6.546	101.886	6278	1.49
39	RR0705-59TC	Trigger	5/26/03	-6.546	101.886	6275	0.00
39	RR0705-59PC	Piston	5/26/03	-6.546	101.886	6275	0.00
40	RR0705-60GC	Gravity	5/26/03	-6.139	101.889	4184	1.73
40	RR0705-61PC	Trigger	5/27/03	-6.139	101.889	4187	2.75

Site #	Core #	Type	Date (GMT)	Latitude dd	Longi-tude dd	Depth (m)	Length (m)
40	RR0705-61TC	Piston	5/27/03	-6.139	101.889	4187	4.28
41	RR0705-62GC	Gravity	5/27/03	-5.610	101.477	3392	1.19
41	RR0705-63TC	Trigger	5/27/03	-5.610	101.477	3397	1.10
41	RR0705-63PC	Piston	5/27/03	-5.610	101.477	3397	2.60
42	RR0705-64GC	Gravity	5/28/03	-4.579	100.858	2751	1.77
42	RR0705-65TC	Trigger	5/28/03	-4.579	100.858	2751	2.68
42	RR0705-65PC	Piston	5/28/03	-4.579	100.858	2751	4.92
43	RR0705-66GC	Gravity	5/29/03	-3.671	100.042	3891	1.62
43	RR0705-67TC	Trigger	5/29/03	-3.671	100.042	3888	2.41
43	RR0705-67PC	Piston	5/29/03	-3.671	100.042	3888	4.87
43	RR0705-68MC	Multi-core	5/29/03	-3.671	100.042	3890	0.00
43	RR0705-69MC	Multi-core	5/29/03	-3.671	100.042	3890	0.00
44	RR0705-71GC	Gravity	5/30/03	-2.981	99.428	4082	1.27
44	RR0705-72TC	Trigger	5/30/03	-2.981	99.428	4082	2.35
44	RR0705-72PC	Piston	5/30/03	-2.981	99.428	4082	4.99
44	RR0705-73MC	Multi-core	5/31/03	-2.981	99.428	4080	0.20
45	RR0705-74MC	Multi-core	5/31/03	-2.133	98.648	4080	0.00
45	RR0705-75MC	Multi-core	5/31/03	-2.133	98.648	3221	0.12
45	RR0705-76TC	Trigger	6/1/03	-2.133	98.648	3221	1.14
45	RR0705-76PC	Piston	6/1/03	-2.133	98.648	3221	4.18

Site #	Core #	Type	Date (GMT)	Latitude dd	Longi-tude dd	Depth (m)	Length (m)
46	RR0705-77TC	Trigger	6/1/03	-1.478	98.155	3778	0.53
46	RR0705-77PC	Piston	6/1/03	-1.478	98.155	3778	2.66
47	RR0705-79TC	Trigger	6/1/03	-0.847	97.794	3833	0.56
47	RR0705-79PC	Piston	6/1/03	-0.847	97.794	3833	4.20
47	RR0705-80MC	Multi	6/2/03	-0.847	97.794	3835	0.08
48	RR0705-81GC	Gravity	6/2/03	-0.663	97.742	3438	0.32
49	RR0705-82MC	Multi	6/2/03	0.130	97.361	3038	0.22
49	RR0705-83TC	Trigger	6/3/03	0.130	97.361	3034	2.09
49	RR0705-83PC	Piston	6/3/03	0.130	97.361	3034	4.87
50	RR0705-85TC	Trigger	6/3/03	1.029	96.800	3337	1.78
50	RR0705-85PC	Piston	6/3/03	1.029	96.800	3337	4.87
50	RR0705-86MC	Multi	6/4/03	1.029	96.800	3337	0.13
51	RR0705-88TC	Trigger	6/4/03	1.312	96.263	5197	0.91
51	RR0705-88PC	Piston	6/4/03	1.312	96.263	5197	4.71
52	RR0705-89TC	Trigger	6/4/03	1.520	96.379	3255	1.48
52	RR0705-89PC	Piston	6/5/03	1.520	96.379	3255	4.38
52	RR0705-90MC	Multi	6/5/03	1.520	96.379	3255	0.13
53	RR0705-91MC	Multi	6/5/03	1.890	95.973	3836	0.14
53	RR0705-92TC	Trigger	6/6/03	1.890	95.973	3836	1.14
53	RR0705-92PC	Piston	6/6/03	1.890	95.973	3836	4.77

Site #	Core #	Type	Date (GMT)	Latitude dd	Longi-tude dd	Depth (m)	Length (m)
54	RR0705-93TC	Trigger	6/6/03	1.721	95.812	5040	1.20
54	RR0705-93PC	Piston	6/6/03	1.721	95.812	5040	4.92
55	RR0705-94TC	Trigger	6/6/03	2.124	95.051	4918	0.00
55	RR0705-94PC	Piston	6/6/03	2.124	95.051	4918	3.81
56	RR0705-95TC	Trigger	6/7/03	2.874	94.206	3418	0.00
56	RR0705-95PC	Piston	6/7/03	2.874	94.206	3418	2.23
57	RR0705-96TC	Trigger	6/7/03	2.934	94.139	3410	1.33
57	RR0705-96PC	Piston	6/7/03	2.934	94.139	3410	4.40
57	RR0705-97MC	Multi	6/7/03	2.934	94.139	3412	0.68
58	RR0705-98TC	Trigger	6/7/03	2.692	94.100	3410	1.22
58	RR0705-98PC	Piston	6/7/03	2.692	94.100	3410	4.77
58	RR0705-99MC	Multi	6/8/03	2.692	94.100	4715	0.24
59	RR0705-102MC	Multi	6/8/03	3.605	93.632	3073	0.22
59	RR0705-103TC	Trigger	6/9/03	3.605	93.632	3073	1.63
59	RR0705-103PC	Piston	6/9/03	3.605	93.632	3073	4.74
60	RR0705-104TC	Trigger	6/9/03	3.872	93.475	3476	1.92
60	RR0705-104PC	Piston	6/9/03	3.872	93.475	3476	4.58
61	RR0705-105TC	Trigger	6/9/03	4.079	93.181	4486	0.55
61	RR0705-105PC	Piston	6/9/03	4.079	93.181	4486	2.75
62	RR0705-106TC	Trigger	6/10/03	3.330	91.939	4142	2.45

Site #	Core #	Type	Date (GMT)	Latitude dd	Longi-tude dd	Depth (m)	Length (m)
62	RR0705-106PC	Piston	6/10/03	3.330	91.939	4142	3.51
63	RR0705-107TC	Trigger	6/10/03	4.327	92.918	4518	1.79
63	RR0705-107PC	Piston	6/10/03	4.327	92.918	4518	0.81
64	RR0705-108TC	Trigger	6/11/03	4.660	93.143	2959	1.28
64	RR0705-108PC	Piston	6/11/03	4.660	93.143	2959	3.70
64	RR0705-109MC	Multi	6/11/03	4.660	93.143	2959	0.06

Cruise Narrative

08:00 2 May, 2007

R/V Revelle alongside the pier at Phuket deep sea port

Loading of heavy coring gear begins, and is completed by 4 May. 5-7 May, science gear loaded aboard and ship fueled. Dates and times are local to Phuket, Thailand.

16:00 7 May

R/V Revelle departed Phuket, Thailand

Transit was southwest toward the northernmost Indonesian part of the 2004 earthquake rupture zone. Transit to Station # 1 was ~ 32 hours via the Nicobar passage.

05:00 9 May

R/V Revelle arrived on station

A brief survey with multibeam and 3.5 kHz sub-bottom was conducted to augment the UK, French and German multibeam data. The site was selected based on these data, and was a small apron fed by a large well developed channel leading from an eroded gully/landslide system on the first ridge of the accretionary wedge. The channel turns southward and is apparently captured by the margin to the east, and a basement normal fault to the west, forming a broad flat floored valley. The channel is here named Aceh Channel.

9 May

Core RR0507-01GC, a small Benthos gravity core was taken in 4380 m of water on the NW part of the small apron. Deployment and recovery were normal, and made on the Hydro wire. Recovery was only ~ 20cm of semi-consolidated clayey silt, with a lower sand contact.

Core RR0507-02GC was a second test core, a Benthos gravity core, several km down channel from station 1. Deployment and recovery were normal. Recovery was ~ 8 cm of material similar to 01GC.

Core RR0507-03PC was a 4" piston core, at the same site as station 2. Deployment and recovery were normal. Recovery was 2m sediment in the trigger core, and ~ 2.5 m of material similar to 01GC on the piston core. Subsequently, core analysis revealed that the trigger core contained repeated sequences, indicating multiple coring of the upper section. Speed into the bottom was slow, and increased for subsequent cores.

Core RR0507-04KC was the first jumbo kasten core of the cruise. The site was down channel from sites 1 and 2, to the southwest, in a water depth of ~ 4580m. All four lead weights were added to the weight stand, for a total head weight of ~ 5200lbs. Pullout was ~ 16,000 lbs, indicating good penetration. Deployment and recovery were normal. On recovery, it was found that the kasten and fully penetrated the bottom, with mud on the barrel almost to the top, however there was no sample. The kasten doors had failed under the sample weight, releasing the sample out the bottom. Subsequently the kasten doors were replaced and reinforced.

10 May

Core RR0507-05PC was a 4" piston core located mid channel between stations 3 and 2. Deployment and recovery were normal. Recovery was 1m sediment in the trigger core, and ~ 2.8 m of material similar to 01GC on the piston core. During this deployment, the bearings in the crane overboard block failed, and the block was subsequently replaced.

Core RR0507-06KC was the second attempted jumbo kasten core of the cruise. The site was down channel from sites 1 and 2, at the same location as 05PC in ~ 4480m. All four lead weights were added to the weight stand, for a total head weight of ~ 5200lbs. This core deployment was aborted when the bearing in the crane base block failed. After rigging the kasten core on the stern, the core was redeployed at the same site. No recovery was made. The core barrel had mud ~ 1m up the side, the doors were tripped, but no sample was inside. The sample may have washed out due to excessive time near the surface.

11 May

Core RR0507-07MC was the first attempted multi core of the cruise. The site was down channel from sites 1 and 2, at the same location as 05PC in ~ 4480m. Deployment and recovery was normal, however there was no recovery. The corer had tripped, and only a small amount of mud was found on one of the shovels. The cause of the non recovery is uncertain. The sediment, based on previous cores, should have been at least 15cm of soft material. The material may have been too soft however to be retained by the vacuum needed to withdraw the sample.

Crane sheave repairs are apparently not possible onboard, we are exploring shipping parts to Padang, or making repairs there.

Core RR0507-08GC was the first jumbo "big bertha" gravity core of the cruise. It is a 4" gravity corer system, using the same weight stand as the piston corer, with a benthos valve at the top. The maximum length of this system is 10'. This site in 4502m of water was not successful, recovering a small quantity of well sorted sand.

12 May

Core RR0507-09GC. This small benthos core in 4541 m of water had a good pullout, but was empty on retrieval, with only some fine grained sediment and several forams on the core catcher.

Core RR0507-10GC. This core was more distal in the same channel system as the previous two cores, up on a high terrace. The recovery was only 23 cm. most likely due to hard fine grained sand.

Core RR0507-11GC. A 4" Big Bertha gravity core was attempted at another site along the same sandy channel system in 4514m of water, but again no recovery. Sandy silt recovered from catcher.

Core RR0507-12GC. Repeat of site of 11GC using thin core catcher and 4" big bertha corer. 50cm recovery.

13 May

Core RR0507-13KC. All gravity coring was shifted to the stern until the Padang port call. The kasten core doors were reinforced, and plastic film sealing was added around the latches. This core had no recovery.

Core RR0507-14GC. Benthos core. Test site on channel levee at mouth of sandy channel of previous cores. A few cm of coarse sand was recovered.

Core RR0507-15GC. Benthos core. Slope basin site in 1911 m of water NW of Nias Island. 32 cm of foram sand were recovered.

Core RR0507-16GC. Repeat of site 15CG with the big bertha corer. A total of 140 cm of foram sand were recovered, three ash layers were also found in the core.

Core RR0507-17KC. A kasten core was attempted at the site of 16GC, with no recovery. Some shell fragments were found in the nose cone of the corer.

14 May

Core RR0507-18GC. Big bertha 4" core taken in the same slope basin, moved slightly more distally from the previous site. Recovery was 315 cm of foram sand with ash layers.

Core RR0507-19GC. This core was taken at the third channel system along the trench from the Indonesian border is 4816 m of water. 67 cm of fine silt and sand were recovered.

Core RR0507-20GC. Big bertha 4" core at the same site as 19GC. Recovery of 222 cm from a channel levee was successful. Water depth 4815 m.

Core RR0507-21GC. A second benthos corer was collected at a lower levee site in 4834 m of water. Similar records were obtained to 20GC, with 40 cm slightly increased grain sizes.

15 May

Core RR0507-22GC. Benthos core in 4983 m of water. 94.6 cm recovery from this trench margin site opposite the Banyak islands. Thin turbidites.

Core RR0507-23GC. Big bertha 4" core in 4973 m of water. 210 cm recovery from this trench margin site opposite the Banyak islands. Thin turbidites.

Core RR0507-24GC. Benthos core in 4976 m of water. 99.5 cm recovery from this trench margin site opposite the Banyak islands.

16 May

Core RR0507-25GC. Benthos core in 5224 m of water. No recovery from this trench margin site opposite Nias island.

17 May

Core RR0507-26GC. Benthos core in 5220 m of water. No from this trench margin site opposite Niase island.

Core RR0507-27GC. Big bertha 4" core in 5214 m of water. 232 cm wiuth thin turbidites. Off Nias Island.

Core RR0507-28GC. Big bertha 4" core in 5240 m of water. No recovery except a small quantity of sand in the core catcher. Between Nias and the Batu islands.

17 May

Core RR0507-29GC. Benthos core in 5302 m of water. Recovery of 139 cm was successful, with thin turbidites from this trench margin site opposite the Batu Islands.

Core RR0507-30GC. Big bertha 4" core at the same site as 34GC in 5436 m of water. Recovery of 181 cm was successful, with thin turbidites. Site is the same as 29GC.

Core RR0507-31GC. Benthos core in 5420 m of water. Recovery of 136.7 cm was successful, with thin turbidites from this trench margin site opposite the Batu Islands.

Core RR0507-32GC. Big bertha 4" core at the same site as 34GC in 5436 m of water. Recovery of 181 cm was successful, with thin turbidites. Site is slightly more proximal and deeper than 31GC.

18 May

Core RR0507-33GC. Benthos core in 5489 m of water. No recovery from this trench margin site opposite the north end of Siberut Island. Most likely hit hard sand.

Core RR0507-34GC. Benthos core in 5462 m of water. Recovery of 85.4 cm was successful, with thin turbidites from this trench margin site opposite the north end of Siberut Island.

Core RR0507-35GC. Big bertha 4" core at the same site as 34GC in 5462 m of water. Recovery of 200.8 cm was successful, with thin turbidites. Site is slightly more distal and shallower than 34GC.

Core RR0507-36KC Jumbo Kasten core was successful recovering 163cm of fine silty/ sand turbidites from the same site as 35GC. Door modifications to the Kasten nose cone were successful at making a better seal of the nose cone. Three nose cone sub-samples were taken of ~ 22cm length. Pullout was 21,221 lbs the highest to date. Site is slightly more distal and shallower than 35GC.

19 May

Core RR0507-37GC. Benthos core in 5492 m of water. Recovery of 88.6 cm from the south end of the basin ponded north of a strand of the Investigator fracture zone, west of the center, was successful, with thin turbidites.

Core RR0507-38GC. Big bertha 4" core at the same site as 37GC in 5511 m of water. Recovery of 186.6 cm from the south end of the basin ponded north of a strand of the Investigator fracture zone , west of the center, was successful, with thin turbidites. Site is slightly east (more proximal) from the benthos site of 37GC.

Core RR0507-39KC was successful recovering 232cm of fine silty/sand turbidites from the same site as 38GC. Door modifications to the Kasten nose cone were successful at making a better seal of the nose cone. Three nose cone sub-samples were taken of ~ 23cm length. Pullout was 21,950 lbs the highest to date.

20 May

Core RR0507-40GC. 122.5 cm of fine silt/mud with thin sand turbidites were recovered from this site just north of a strand of the Investigator fracture zone. The site is in the NW of a sediment catchment pond created by the impingement of the fracture zone on the trench axis.

Core RR0507-41GC. Big bertha 4" core at the same site as 40GC in 5540 m of water. Recovery of 162 cm from the basin, west of the center, was successful, with thin turbidites.

21 May

Padang, Sumatra, Indonesia port call

The ship transited to the port of Padang, Teluk Bayur on the morning of 21 May, arriving at 0630. Three science party members and one film cameraman departed, and three new science party members were signed aboard. Repair parts were taken aboard for the fairlead sheaves for the starboard crane.

22 May

Core RR0507-42GC. A benthos gravity core was attempted in a slope basin at a depth of 1150 m in a slope basin just west of the south end of Siberut island. This core recovered ~ 10 cm of coarse foram sand and mud.

23 May

Core RR0507-43GC. 80m cm of fine silt/mud with thin sand turbidites were recovered from this site just north of a strand of the Investigator fracture zone. The site is in the center of a sediment catchment pond created by the impingement of the fracture zone on the trench axis.

Core RR0507-44MC. Same site as above, the multicore failed, recovering only 2-4 cm of mud. Penetration of 20-25 cm indicated by mud streaks on the outside of the tubes. All but one tube slightly misaligned with the closed doors, possibly allowing sediment to escape.

Core RR0507-45PC. Same site as above. ~ 5.8 m of sediment recovered on the piston core, and ~ 1m recovered in the trigger core. Pullout light at ~ 13,000 lbs. The trigger core includes several sand turbidites and fine silty muds. The trigger penetrated the

bottom twice, with seafloor oxidation at the top, and ~ 15 cm above the bottom of the core. Many of the turbidites in the lower sections of this core are ash bearing.

Core RR0507-46GC. Benthos core, southern part of the Investigator fracture zone. Small sediment ponds are located between the main and smaller NE trending basement ridges of the fracture zone. This site is on the southeastern side of one of the easternmost strands of the Investigator fracture zone. Core taken in well stratified turbidites imaged on the 3.5 kHz profiler and recovered 1.8 m of thin turbidite silty sands.

Core RR0507-47PC. Eastern part of the Investigator fracture zone. This site is in the southern side of one of the southernmost spurs of the Investigator ridge. Core taken in well stratified turbidites imaged on the 3.5 kHz profiler at the same site as 46GC, water depth 5726m. Recovered 1 m of thin turbidites silty sands in the trigger core, and ~3m in the piston core. Corer completely penetrated and the weight stand had mud inside. Pullout was 17,500 lbs.

24 May

Core RR0507-48GC. Benthos core north of an unnamed ridge in a sediment pond defined by the subducting ridge. Recovery of 168 cm included sand turbidites.

Core RR0507-49PC. 4" piston core north of an unnamed ridge in a sediment pond defined by the subducting ridge. Recovery of 257 cm in the trigger core and 397 cm in the piston core included sand turbidites.

25May

Core RR0507-50GC. Benthos core north of an unnamed ridge in a sediment pond defined by the subducting ridge. Recovery of 107 cm included sand turbidites.

Core RR0507-51GC. Benthos core south of an unnamed ridge in a sediment pond defined by a basement normal fault impinging on the trench. No recovery except small amount of soft sediment. Probable hard sand substrate.

Core RR0507-52GC. Benthos core south of an unnamed ridge in the flank of a protothrust ridge formed over a reactivated normal fault impinging on the trench. 14 cm of fine sand and mud recovered.

Core RR0507-53GC. Benthos core south of an unnamed ridge south of several down to the south normal faults impinging on the trench. 20 cm of mud recovered. This and previous benthos had sediment laden water to the top for unknown reasons. Water depth 6060m.

Core RR0507-54GC. Benthos core south of an unnamed ridge south of several down to the south normal faults impinging on the trench. Same site as previous. Benthos valve replaced. 40 cm of mud recovered. Benthos valve replacement solved sediment laden water problem. Water depth 6060m.

26 May

Core RR0507-55PC. Piston core south of an unnamed ridge south of several down to the south normal faults impinging on the trench. Moved site 6nm north from previous. 260 cm thick sand turbidites recovered, trigger core empty. Water depth 6046m.

Core RR0507-56GC. Benthos core at new site, water depth 6060m. 40cm of muddy silt recovered, core sample damaged on retrieval.

Core RR0507-57PC. Water depth 6069m. Four section, 491 cm were recovered from the trench axis off Enganno island. Winch control tripped offline for ~ 3 minutes while the core was in the bottom. This core had excellent recovery of sand turbidites and the seafloor surface. No recovery from the trigger core for unknown reasons.

27 May

Core RR0507-58GC. Benthos core at new site off Enganno, water depth 6279m. 146 cm of muddy silt recovered.

Core RR0507-59PC. Water depth 6275m. 230 cm were recovered in the trigger core from the trench axis off Enganno island. Winch control tripped offline 6 times while the core was in the water due to sea state and surging of the winch from ship motion at the stern. A pre-trip occurred at ~ 5000m depth, with a 23,2000 lb load. Shock absorbing piston may have prevented a wire break. The trigger core had excellent recovery of sand turbidites and the seafloor surface. No recovery from the piston core due to the pre-trip.

Core RR0507-60GC. Benthos core at new slope basin site off Enganno, water depth 4184m. 168 cm of muddy silt and foram sand recovered. Forams eroded, most likely near CCD for late Holocene.

28 May

Core RR0507-61PC. Water depth 4184m. A full trigger core of cm was recovered from a slope basin off Enganno island. Winch control tripped offline several times and the core freewheeled into the bottom from 80m. Again this was due to sea state and surging of the winch from ship motion at the stern, and temperature of the winch system (seawater cooled) may have been a factor. The trigger and piston core had excellent recovery of sand turbidites, thought the trigger overpenetrated and did not recover the seafloor surface. The piston core recovered 428 cm, the trigger core recovered 275 cm.

Core RR0507-62GC. Benthos core at new slope basin site between Enganno and South Pagai, water depth 3395m. 119.2 cm of muddy silt and foram sand recovered.

Core RR0507-63PC. Water depth 3350m. A trigger and piston core were recovered from a slope basin between Enganno island and South Pagai. The trigger and piston core had excellent recovery of sand turbidites. The piston core recovered 260 cm, the trigger recovered 110 cm.

29 May

Core RR0507-64GC. Benthos core at new slope basin site between Enganno and South Pagai, water depth 2751m. Basin is fed by a large low-stand channel system filling a series of spill-over basins from what would have been an exposed island during the last glacial maximum. Possible Holocene Pleistocene boundary from muddy to very sandy ~ 4m in this basin. 176 cm of muddy silt and foram sand recovered. Multiple sand turbidites over foram sand and hemipelagic with possible flame load structures apparent.

Core RR0507-65PC. Piston core at same slope basin site between Enganno and South Pagai, water depth 2751m. Basin is fed by a large low-stand channel system filling a series of spill-over basins from what would have been an exposed island during the last glacial maximum. Possible Holocene-Pleistocene boundary, from muddy to very sandy sediment, at ~4m beneath the sea floor in this basin. Core stuck in the bottom for 18 hours. Pulled to over 28000 lbs to no effect, let the ship try to rock it out of the bottom under average pull of ~ 24000 lbs for 15 hours. Moving ship 500 m off station to create a 10 degree wire angle succeeded in extracting the core without damage to the system, although the wire below 2800m was overloaded. Trigger core was over penetrated, with mud in the benthos valve, core barrel full at 268 cm. Piston core also recovered 492 cm although it contained several voids that may be suction voids, or may be sand liquefaction washouts. Piston core penetrated probable Holocene section in the possible Pleistocene age fine well-sorted mature sands which were likely what prevented the pullout. Core bottomed in a large ash layer visible in the sub-bottom profile.

30 May

Core RR0507-66GC. Slope basin off the south end of South Pagai island. 162 cm of muddy silt and foram sand recovered. Multiple sand turbidites over foram sand and hemipelagic sediment. Water depth 3891m

Core RR0507-67PC. Slope basin off the south end of South Pagai island. 487 cm of muddy silt and foram sand recovered in the PC, 241 recovered in the TC. Multiple sand turbidites over foram sand and hemipelagic sediment. Water depth 3891m

Core RR0507-68MC. Slope basin off the south end of South Pagai island. No recovery in the multicore, reasons unknown. Water depth 3891m

31 May

Core RR0507-69MC. Slope basin off the south end of South Pagai island. No recovery in the multicore, upon idssasembly of the multicore, the pneumatic washer was found to be detached from the piston. Likely all multicores thus far have pre-tripped. Water depth 3891m.

Core RR0507-70PC. Reoccupation of trench site at station 33. Off South Pagai island. 509cm of muddy silt and foram sand recovered in the PC, 181 recovered in the TC. Multiple sand turbidites over foram sand and hemipelagic sediment. Water depth 5805m. Bow thruster offline, maintaining position with main engines. Winch tripped offline 6 times on descent.

1 June

Core RR0507-71GC. New slope basin site off Sipora island. 126.5 cm of muddy silt and foram sand recovered. Multiple sand turbidites over foram sand and hemipelagic. Water depth 4089m. Bow thruster offline, maintaining position with main engines.

Core RR0507-72PC. New slope basin site off Sipora island, same site as 71GC. 499 cm of muddy silt and foram sand recovered in the PC, 239.5 recovered in the TC. Multiple sand turbidites over foram sand and hemipelagic. Water depth 4089m. Bow thruster offline, maintaining position with main engines. Winch tripped offline several times on descent. Good recovery of eroded foram bearing hemipelagite between events.

Core RR0507-73MC. Multi-core in a slope basin site off Sipora Island, same site as 71GC. 8 tubes; full recovery of ~ 18-20cm each tube of undisturbed seafloor. Slight leakage of two tubes on recovery. Repairs to hydraulic tube were successful. Soft sediment wooden "shoes" for the multicore, installed for the soft Santa Barbara basin were also removed. Water depth 4089m.

2 June

Core RR0507-74MC. Multi-core in a new slope basin site off south Siberut island. No Recovery.

Core RR0507-75MC. Slope New slope basin site off south Siberut Island. 8 tube full recovery of 10-12 cm each tube of undisturbed seafloor. Water depth 3221m.

Core RR0507-76PC. New slope basin site off Siberut Island, same site as 75MC. 418 cm of muddy silt and foram sand recovered in the PC, 114 recovered in the TC. Multiple seafloor surfaces in the TC. Multiple sand turbidites over foram sand and hemipelagic. Water depth 3221m. Bow thruster offline, maintaining position with main engines.

Core RR0507-77PC. New slope basin site off northern Siberut Island. 265 cm of muddy silt and foram sand recovered in the PC, 53 cm recovered in the TC. Multiple sand turbidites over foram sand and hemipelagic. Water depth 3778m. Bow thruster offline, maintaining position with main engines.

3 June

Core RR0507-78PC. Piston core at station 24 in the trench axis. 444 cm of muddy silt and foram sand recovered in the PC, 151.5 recovered in the TC. Multiple sand turbidites. Water depth 5455m. Bow thruster offline, maintaining position with main engines.

Core RR0507-79PC. New slope basin site off the Batu islands. 419.5 cm of muddy silt and foram sand recovered in the PC, 56 recovered in the TC. Multiple sand turbidites over foram sand and hemipelagic. Water depth 3833m. Bow thruster offline, maintaining position with main engines.

Core RR0507-80MC. New slope basin site off the Batu islands, same site as 79PC. 7-9.5 cm of muddy silt and foram sand recovered in 6 tubes of the multi-core. Single sand

turbidite over foram sand and hemipelagic. Water depth 3833m. Bow thruster offline, maintaining position with main engines.

Core RR0507-81GC. Benthos gravity core. Slope basin off the Batu islands island. 31.5 cm of muddy silt and foram sand recovered. Multiple sand turbidites over foram sand and hemipelagic. Water depth 3445m

4 June

Core RR0507-82MC. New slope basin between Nias and the Batu islands. 19-23 cm of muddy silt and foram sand recovered in 7 of 8 tubes of the multi-core. Single sand tubiditee over foram sand and hemipelagic. Water depth 3033m. Bow thruster offline, maintaining position with main engines.

Core RR0507-83PC. New slope basin between Nias and the Batu islands, same site at 82MC. 487 cm of muddy silt and foram sand recovered in the TC, 208.5 cm in the PC. Sand turbidites over foram sand and hemipelagic sediment. Water depth 3033m. Bow thruster offline, maintaining position with main engines.

Core RR0507-84PC. Reoccupation of station 19, a trench site off southern Nias. 344.2 cm of muddy silt and thin foram sand recovered in the TC, 110.8 cm in the PC. Thin sand turbidites. Water depth 5303m. Bow thruster offline, maintaining position with main engines.

5 June

Core RR0507-85PC. New basin site off southern Nias. 178 cm of muddy silt and thin foram sand recovered in the TC, 486.5 cm in the PC. Thin sand turbidites. Water depth 3307m. Bow thruster offline, maintaining position with main engines.

Core RR0507-86MC. New basin site off southern Nias. 11-15.5 cm of muddy silt and foram sand recovered in 6 of 8 tubes of the multi-core. Single sand turbidite over foram sand and hemipelagic. Water depth 3337m. Bow thruster offline, maintaining position with main engines.

Core RR0507-87PC. Reoccupation of station 17, a trench site off Nias. 76.9 cm of muddy silt and thin foram sand recovered in the TC, 502 cm in the PC. Thin sand turbidites. Water depth 3307m. Bow thruster offline, maintaining position with main engines.

Core RR0507-88PC. New trench station between original stations 14 and 17. Located just south in the trench axis of an older landslide with blocks covering the trench floor. Small fans and channels entering the trench just to the east. On-lap of trench fill indicates a relatively old slide. Site located off Nias Island. 471 cm of muddy silt and thin foram sand recovered in the TC, 90.5 cm in the PC. Thin sand turbidites. Water depth is 5190m. Bow thruster offline, maintaining position with main engines.

Core RR0507-89PC. New basin station between original stations 14 and 17. Located in a small isolated basin between major channel systems coming from Simeulue. 147.5

cm of muddy silt and thin foram sand recovered in the TC, 438 cm in the PC. Thin sand turbidites. Water depth is 3256m. Bow thruster offline, maintaining position with main engines.

6 June

Core RR0507-90MC. New basin station between original stations 14 and 17, same site as 89PC. Located in a small isolated basin between major channel systems coming from Simeulue. 9-20 cm of muddy silt and thin foram sand recovered in 8 of 8 tubes. Tubes 6 and 7 recovered more material, penetrated two turbidites, possible upper sand from the 2005 Nias earthquake apparent, and not sampled by the trigger core at the same site. Water depth is 3256m. Bow thruster offline, maintaining position with main engines.

Core RR0507-91MC. New basin station between original stations near the latitude of station 14. Located in a small isolated basin between major channel systems coming from Simeulue. 12-16 cm of muddy silt and thin foram sand recovered in 8 of 8 tubes. Water depth is 3836 m. Bow thruster offline, maintaining position with main engines.

Core RR0507-92PC. New basin station between original stations near the latitude of station 14. Located in a small isolated basin between major channel systems coming from Simeulue, same station as 91MC. 114 cm of muddy silt and thin foram sand recovered in the trigger core. 476.5 cm recovered in the piston core. Water depth is 3836m. Bow thruster offline, maintaining position with main engines.

Core RR0507-93PC. New trench axis station near the latitude of station 14. Located on the flank of a small fan coming from a channel leading from the frontal thrust. 120.2 cm of muddy silt and thin foram sand recovered in the trigger core. 491.5 cm recovered in the piston core. Water depth is 5038m. Bow thruster offline, maintaining position with main engines.

7 June

Core RR0507-94PC. New trench axis station near station 12. Located on the northern flank of a small fan coming from a channel leading from the frontal thrust. Site is just on the levee of an obvious incised and sand filled channel. No sediment recovered in the trigger core, 381 cm recovered in the piston core. Water depth is 4918m. Bow thruster offline, maintaining position with main engines.

Core RR0507-95PC. New basin station near station 12. Located on the northern flank of a small fan coming from a channel leading from a 1000m high ridge. No sediment recovered in the trigger core, 222.5 cm recovered in the piston core. Water depth is 3417 m. Bow thruster offline, maintaining position with main engines.

8 June

Core RR0507-96PC. New basin station near station 12. Located on the western flank of a small fan coming from a channel leading from a 1000m ridge. Isolated from main basin by secondary mid-basin structure. 132.7 cm sediment recovered in the trigger core, 440 cm recovered in the piston core. Water depth is 3410 m. Bow thruster offline, maintaining position with main engines

Core RR0507-97MC. New basin station near station 12. Located on the western flank of a small fan coming from a channel leading from a 1000m ridge. Isolated from main basin by secondary mid-basin structure. 63-69 cm sediment recovered in 7 of 8 tubes, no recovery in tube #4. Water depth is 3410 m. Bow thruster offline, maintaining position with main engines.

Core RR0507-98PC. Piston core at new trench site north of Simeulue. Located just south of an older landslide block partially blocking the trench, and on northern flank of an active fan fed by channel system leading out from the frontal thrust. 477 cm of muddy silt and thin foram sand recovered in the piston, 121.5 cm in the trigger. Water depth is 4716 m. Bow thruster offline, maintaining position with main engines.

9 June

Core RR0507-99MC. Multi-core at new trench site north of Simeulue. Located just south of an older landslide block partially blocking the trench, and on northern flank of an active fan fed by channel system leading out from the frontal thrust. 22-23 cm of muddy silt and thin foram sand recovered in 8 of 8 tubes. Water depth is 4716 m. Bow thruster offline, maintaining position with main engines.

Core RR0507-100MC. Multi-core at station 11 to record upper section possibly missing from earlier core at this station. 4-10cm of muddy silt and thin foram sand recovered in 3 of 8 tubes, 0 to 0.5 cm in the other tubes. Water depth is 1823 m. Bow thruster offline, maintaining position with main engines.

Core RR0507-101GC. Benthos gravity core at station 11 to record upper section possibly missing from earlier core at this station. 52.5 cm of muddy silt and thin foram sand recovered. Water depth is 1823 m. Bow thruster offline, maintaining position with main engines.

Core RR0507-102MC. New basin station between original stations near the latitude of station 8. Located in a small isolated perched basin. 20-25 cm of muddy silt and thin foram sand recovered in 8 of 8 tubes. Water depth is 3041m. Bow thruster offline, maintaining position with main engines.

10 June

Core RR0507-104PC. Piston core at new basin site north of Simeulue. Isolated basin site. 457 cm of muddy silt and thin foram sand recovered in the piston, 192.4 cm in the trigger. Water depth is 3476 m. Bow thruster offline, maintaining position with main engines.

Core RR0507-105PC. Piston core at trench site north of Simeulue. Northern flank of a small fan growing into the trench floor out of a channel mouth in a landward vergent thrust ridge. Just south of an older slump deposit. 274.5 cm of muddy silt and thin foram sand recovered in the piston, 54.5 cm in the trigger. Water depth is 4486 m. Bow thruster offline, maintaining position with main engines.

11 June

Core RR0507-106PC. Piston core at distal channel site north of Simeulue. Site located from BGR multibeam near the eastern flank of the Ninety East Ridge. Channel leads north into Indian waters on the Nicobar fan. Ultimate source unknown. Site on the eastern lower levee of a two levee system. Section is expanded in the channel thalweg, but coring capabilities limited core length and so a levee site was selected. 351 cm of hemipelagic and thin foram sand recovered in the piston, 245 cm in the trigger. Water depth is 4142 m. Bow thruster offline, maintaining position with main engines.

Core RR0507-107PC. Piston core near station 3 north of Simeulue on the trench. Site located from 3.5 kHz records on the western trench flank, 5m above trench floor. Core pre-tripped in the water, only 80 cm of disturbed sand, muddy silt and thin foram sand recovered in the piston, 179 cm in the trigger. Water depth is 4518 m. Bow thruster offline, maintaining position with main engines.

12 June

Core RR0507-108PC. Piston core at new basin site north of Simeulue. Site located in piggyback basin fed from probable relict Pleistocene channel system. 369.5 cm of muddy silt and coarse sand recovered in the piston, 128 cm in the trigger. Water depth is 2959 m. Bow thruster offline, maintaining position with main engines.

Core RR0507-109MC. Multi-core at new basin site north of Simeulue. Site located from 3.5 kHz records on the western trench flank, 5m above trench floor. 6-7.5 cm of muddy silt and thin foram sand recovered in 6 of 8 tubes, 2 tubes empty. Water depth is 2959 m. Bow thruster offline, maintaining position with main engines.

References Cited

Adam, J., D. Klaeschen, N. Kukowski, and E. Flueh, (2004), Upward delamination of Cascadia Basin sediment infill with landward frontal accretion thrusting caused by rapid glacial age material flux: Tectonics, v.23, p. TC3009.

Ammon, C. J., C. Ji, H.K. Thio, D. Robinson, S. Ni, V. Hjorleifsdottir, H. Kanamori, T. Lay, S. Das, D. Helmberger, G. Ichinose, J. Polet, D. Wald, (2005), Rupture Process of the 2004 Sumatra-Andaman Earthquake: Science, v.308, (5725), pp.1133-1139.

Adams, J., 1990, Paleoseismicity of the Cascadia subduction zone: evidence from turbidites off the Oregon-Washington margin: Tectonics, v. 9, p 569-583.

Abdeldayem, A. L., Ikehara, K., and Yamazaki, T., 2004, Flow path of the 1993 Hokkaido-Nansei-oki earthquake seismotrubidite, southern margin of the Japan sea north basin, inferred from anisotropy of magnetic susceptibility: Geophysical Journal International, v. 157, p. 15-24.

Anastasakis, G.C., and Piper, D.J.W., 1991, The character of seismo-turbidites in the S-1 sapropel, Zakinthos and Strofadhes basins, Greece: Sedimentology, v. 38, p. 717-733.

Ando, M., and Balazs, E.I., 1979, Geodetic evidence for aseismic subduction of the Juan de Fuca plate: Journal of Geophysical Research, v. 84, p. 3023-3027.

Atwater, B.F., 1987, Evidence for great Holocene earthquakes along the outer coast of Washington State: Science, v. 236, p. 942-944.

Atwater, B.F., 1992, Geologic evidence for earthquakes during the past 2000 years along the Copalis River, southern coastal Washington: Journal of Geophysical Research, v. 97, p. 1901-1919.

Atwater, B.F., Nelson, A.R., Clague, J.J., Carver, G.A., Yamaguchi, D.K., Bobrowsky, P.T., Bourgeois, J., Darienzo, M.E., Grant, W.C., Hemphill-Haley, E., Kelsey, H.M., Jacoby, G.C., Nishenko, S.P., Palmer, S.P., Peterson, C.D., and Reinhart, M.A., 1995, Summary of coastal geologic evidence for past great earthquakes at the Cascadia subduction zone: Earthquake Spectra, v. 11, p. 1-18.

Atwater, B.F., and Hemphill-Haley, E., 1996, Preliminary estimates of recurrence intervals for great earthquakes of the past 3500 years at northeastern Willipa Bay, Washington, USGS Open File Report 96001, 88p.

Bacon, C.R., 1983, Eruptive history of Mount Mazama and Crater Lake Caldera, Cascade Range, U.S.A.: Journal of Volcanology and Geothermal Research, v. 18, p. 57-115.

Bandopadhyay, A., and Bandopadhyay, R. R., 1999, Thermogenic Hydrocarbons in the Mid-proximal Bengal Fan, West of the Andaman -Nicobar Islands: Marine Georesources and Geotechnology, v. 17, p. 1-16.

Barnes, P. M., B. Davy, et al. (2002). «Frontal accretion and thrust wedge evolution under very oblique plate convergence: Fiordland Basin, New Zealand.» Basin Research **14**(4): 439-466.

Bilek, S.L., and T. Lay, (2002), Tsunami earthquakes possibly widespread manifestations of frictional conditional stability, Geophys. Res. Let., 2(14), 10.1029/2002GL015215.

Bock, Y., Prawirodirdjo, L., Genrich, J. F., Stevens, C. W., McCaffrey, R., Subarya, C., Puntodewo, S. S. O., and Calais, E., 2003, Crustal motion in Indonesia from Global Positioning System measurements: Journal of Geophysical Research, v. 108, p. doi:10.1029/2001JB000324.

Brachfeld, S. and Banerjee, S.K, 2000, A new high-resolution geomagnetic relative paleointensity record for the North American Holocene: A comparison of sedimentary and absolute intensity data, J. Geophys. Res. 105, 821-834.

Burgmann, R., M. G. Kogan, G. S. Steblov, G. Hilley, V. E. Levin, and E. Apel, 2005, Interseismic coupling and asperity distribution along the Kamchatka subduction zone: Journal of Geophysical Research, v. 110, no. B07405, p. doi:10.1029/2005JB003648.

Byrne, D. E., D. M. Davis, and L. R. Sykes, (1988), Local and maximum size of thrust earthquakes and the mechanics of the shallow region of subduction zones, Tectonics, v. 7, pp. 833-857.

Byrne, D.E., W. Wang, and D.M. Davis, (1993), Mechanical Role of Backstops in the Growth of Forearcs: Tectonics, v. 12, pp 123-144.

Carlson, P.R., 1967, Marine Geology of Astoria Submarine Canyon: Ph.D. Thesis, Corvallis, Oregon State University, 259 p.

Chesner, C. A., 1988, Thesis, Michigan Technology University, p. 428.

Constable, C.G., Johnson, J. L., and Lund, S. P., 2000, Global geomagnetic field models for the past 3000 years: transient or permanent flux lobes?. Phil. Trans. R. Soc. Series A. 991-1008.

Channell, J.E.T., 1999, Geomagnetic paleointensity and directional secular variation at Ocean Drilling Program (ODP) Site 984 (Bjorn Drift) since 500 ka: Comparisons with ODP Site 983 (Gardar Drift). J. Geophys. Res., 104, 22,937-22,951.

Chen Ji, 2005, personal communication.

Curray, J. R., 2004, Tectonics and history of the Andaman Sea Region: Journal of Asian Earth Sciences, in press.

Darienzo, M.E., and Peterson, C.D., 1990, Episodic tectonic subsidence of late Holocene salt marshes, northern Oregon central Cascadia margin: Tectonics, v. 9, p. 1-22.

Davis, D., Suppe, J., and Dahlen, F.A., 1983, Mechanics of fold-and-thrust belts and accretionary wedges: Journal of Geophysical Research, v. 88, p. 1153-1172.

DeMets, C., Gordon, R.G., Argus, D.F., and Stein, S., 1994, Effect of recent revisions to the geomagnetic reversal time scale on estimates of current plate motions: Geophysical Research Letters, v. 21, p. 2191-2194.

Duncan, J.R., Fowler, G.A., and Kulm, L.D., 1970, Planktonic Foraminiferan-Radiolarian ratios and Holocene-Late Pleistocene deep-sea stratigraphy off Oregon: Geological Society of America Bulletin, v. 81, p. 561-566.

Field, M. E., Gardner, J. V., Jennings, A. E., and Edwards, B. D., 1982, Earthquake-induced sediment failures on a 0.25 degree slope: Klamath River Delta, California: Geology, vol. 10, p. 542-546.

Field, M. E., 1984, The Submarine Landslide of 1980 off Northern California: U. S. Geological Survey, Circular 938, p. 65-72.

Fisher, D., D. Mosher, J.A. Austin, S.P. Gulick, T. Masterlark, K. and Moran, (2007), Active deformation across the Sumatran forearc over the December 2004 Mw9.2 rupture: Geology, v. 35, p. 99-102.

Fitch, T. J., 1972, Plate convergence, transcurrent faults, and internal deformation adjacent to southeast Asia and the western Pacific: J. Geophys. Res., v. 77, p. 4432-4460.

Flueh ER, N. Vidal, C.R. Ranero, A. Hojka, R. von Huene, J. Bialas, K. Hinz, D. Cordoba, Zelt C. Dañobeitia, (1998) Seismic investigation of the continental margin off- and onshore Valparaiso, Chile: Tectonophysics, v. 288:251–263

France-Lanord, C, Spiess, V., Molnar, P., Curray, J. 2000 Summary on the Bengal Fan An introduction to a drilling proposal.

Gallet, Y., Genevey, A., Courtillot, V. On the possible occurrence of 'archaeomagnetic jerks' in the geomagnetic field over the past three millennia. Earth and Planetary Science Letters, in press.

Garfield, N., Rago, T. A., Schnebele, K. J., and Collins, C. A., 1994, Evidence of a turbidity current in Monterey Submarine Canyon associated with the 1989 Loma Prieta earthquake: Continental Shelf Research, vol. 14, no. 6, p. 673-686.

Goldfinger, C., Kulm, L. D., Yeats, R. S., Appelgate, B., MacKay, M., and Moore, G. F., 1992, Transverse structural trends along the Oregon convergent margin: implications for Cascadia earthquake potential: Geology, v. 20, p. 141-144.

Goldfinger, C., Kulm, L. D., Yeats, R. S., McNeill, L., and Hummon, C., 1997, Oblique strike-slip faulting of the central Cascadia submarine forearc: Journal of Geophysical Research, v. 102, no. B4, p. 8217-8243.

Goldfinger, C., and Nelson, C.H., 2005, Holocene Recurrence of Cascadia Great Earthquakes based on the Turbidite Event Record: re-submitted to Nature 2/05.

Goldfinger, C., Nelson, C. H., and Johnson, J. E., 2001, Holocene Seismicity of the Northern San Andreas Fault Based on the Turbidite Event Record: Seismological Research Letters, v. 72.

Goldfinger, C., Nelson, C. H., and Johnson, J. E., 2001, Temporal patterns of turbidites offshore the Northern San Andreas Fault and correlation to paleoseismic events onshore: EOS, Transactions of the American Geophysical Union, v. 82, p. F934.

Goldfinger, C. Nelson, C. H., Johnson, J., 2003a, Holocene Earthquake Records From the Cascadia Subduction Zone and Northern San Andreas Fault Based on Precise Dating of Offshore Turbidites Annual Reviews of Geophysics, v. 31, p. 555-577.

Goldfinger, C., Nelson, C.H., and Johnson, J.E., 2003b, Deep-Water Turbidites as Holocene Earthquake Proxies: The Cascadia Subduction Zone and Northern San Andreas Fault Systems: Annali Geofisica, v. 46, p. 1169-1194.

Goldfinger, C., Nelson, C.H., and Johnson, J.E., 2004a, Deep-Water Turbidites as Holocene Earthquake Proxies: The Northern San Andreas Fault System, San Andreas Fault Workshop: USGS, Menlo Park California.

Goldfinger, C., Nelson, C.H., Johnson, J.E., Morey-Ross, A., Eriksson, A., Karabanov, E., and Chaytor, J., 2004b, Holocene earthquake records from the Cascadia subduction zone and northern San Andreas Fault based on precise dating of offshore turbidites, *in* Satake, K., Goldfinger, C., ed., Workshop on Turbidites as Earthquake Recorders: Tsukuba, Japan, AIST, Geological Survey of Japan.

Goldfinger, C., Nelson, C. H., Johnson, J. E., Arsenault, M. A., Eriksson, A., Karabanov, E., and Chaytor, J., 2004, Physical Property Correlations from Cascadia Great Earthquakes: What Are They Telling Us About The Triggering Events?: Eos Trans. AGU.

Goldfinger, C., and L.C. McNeill, (2006), Sumatra and Cascadia: Parallels Explored: Eos Trans. AGU, Fall Meet. Suppl., Abstract U53A-0026, v. 87.

Goldfinger, C., Morey, A.E., Nelson, C.H., Gutierrez-Pastor, J., Johnson, J.E., Karabanov, E., Chaytor, J., and Ericsson, A., (2007a), Rupture Lengths and Temporal History of Significant Earthquakes on the Offshore and North Coast Segments of the Northern San Andreas Fault Based on Turbidite Stratigraphy: Earth and Planetary Science Letters, v. 254, p. 9-27.

Goldfinger, C., (2007b), Constraining stress gradients in the Cascadia forearc: results from investigations of structural, seismologic, and borehole data. Final report, DOGAMI integrated tsunami modeling of the central Cascadia margin, 19p.

Gorsline, D.S., De Diego, T., and Nava-Sanchez, E.H., 2000, Seismically triggered turbidites in small margin basins: Alfonso Basin, Western Gulf of California and Santa Monica Basin, California Borderland: Sedimentary Geology, v. 135, p. 21-35.

Griggs, G.B., 1969, Cascadia Channel: the Anatomy of a Deep-Sea Channel: Ph.D. Thesis, Corvallis, Oregon State University, 183 p.

Griggs, G.B., Carey, A.G., and Kulm, L.D., 1969, Deep-sea sedimentation and sediment-fauna interaction in Cascadia Channel and on Cascadia Abyssal Plain: Deep-Sea Research, v. 16, p. 157-170.

Griggs, G.B., and Kulm, L.D., 1970, Sedimentation in Cascadia Deep-Sea Channel: Geological Society of America Bulletin, 81, 1361-1384.

Grilli, S.T., M. Ioulalalen, J. Asavanant, J.T. Kirby, F. Shi, P. Watts, F. Dias, (2005), Modeling the 12/26/04 Indian Ocean Tsunami generation, propagation, and coastal impact: Integration of SEATOS cruise and other geophysical data, Eos Trans. AGU, 86 (52), Fall Meet Suppl.,

Gulick, S. P. S., N. L. B. Bangs, T. H. Shipley, Y. Nakamura, G. Moore, and S. Kuramoto, (2004), Three-dimensional architecture of the Nankai accretionary prism's imbricate thrust zone off Cape Muroto, Japan: Prism reconstruction via en echelon thrust propagation: J. Geophys. Res., 109, B02105, doi:10.1029/2003JB002654.

Gulick, S. P. S., A. M. Meltzer, and S. H. Clarke, Jr., (1998), Seismic structure of the southern Cascadia subduction zone and accretionary prism north of the Mendocino triple junction: J. Geophys. Res., 103(B11), 27,207-27,222.

Gutscher, M.A., D. Klaeschen, E. Flueh, J. Malavielle, (2001), Non-Coulomb wedges, wrong-way thrusting, and natural hazards in Cascadia, Geology, v.25, pp.379-382.

Guyodo, Y. Channell, J.E.T., and Thomas, R., 2002, Deconvolution of u-channel paleomagnetic data near geomagnetic reversals and short events. Geophys. Res. Letters, 29(17), 1845, doi:10.1029/ 2002GL014927.

Hagstrum, J. T, B. F. Atwater, B. L. Sherrod, 2004, Paleomagnetic correlation of late Holocene earthquakes among estuaries in Washington and Oregon. Geochemistry, Geophysics, Geosystems, Volume 5, Q10001, doi:10.1029/2004GC000736.

Henstock, T.J., L.C. McNeill, and J.R. Tappin, (2006), Seafloor morphology of the Sumatran subduction zone: Surface rupture during megathrust earthquakes?: Geology, v.34, pp. 485-488.

Hodell, D. A., M. Brenner, J. H. Curtis, and T. Guilderson, 2001, Solar forcing of drought frequency in the Maya lowlands. Science 292, 1367-1370.

Horng, C.-S., Lee, M.-Y., P¨alike, H., Wei, K.-Y., Liang, W.-T., Iizuka, Y., and Torii, M., 2002, Astronomically calibrated ages for geomagnetic reversals within the Matuyama chron: Earth Planets Space, v. 54, p. 679–690.

Hu F. S., D. Kaufman, Y. Sumiko, D.Nelson, A. Shemesh,Y. Huang,J. Tian, G, Bond, B. Clegg, T. Brown, 2003, Cyclic Variation and Solar Forcing of Holocene Climate in the Alaskan Subarctic. Science 301, 1890-1893.

Hughen, K. S. Lehman, J. Southon,J. Overpeck, O. Marchal, C. Herring,1 J. Turnbull, 2004, 14C Activity and Global Carbon Cycle Changes over the Past 50,000 Years. Science, 303, 202-207.

Hyndman, R. D. and K. Wang, (1993), Thermal constraints on the zone of major thrust earthquake failure: The Cascadia subduction zone, J. Geophys. Res., v.98, 2,039-2,060.

Inouchi, Y., Kinugasa, Y., Kumon, F., Nakano, S., Yasumatsu, S., and Shiki, T., 1996, Turbidites as records of intense palaeoearthquakes in Lake Biwa, Japan: Sed. Geol., v. 104, p. 117-125.

Ikehara, K., 2004, Estimation of recurrence intervals of large earthquakes using deep-sea turbidites around Japan, *in* Satake, K., Goldfinger, C., ed., Workshop on Turbidites as Earthquake Recorders: Tsukuba, Japan, AIST, Geological Survey of Japan.

Iwaki, H., Hayashida, A., Kitada, N., Ito, H., Suwa, S., and Takemura, K., 2004, Stratigraphic correlation of samples from the Osaka Bay off Kobe based on magnetic properties and its implication for tectonic activity of teh Osaka-wan fault for the last 6300 years: Eos Transactions American Geophysical Union, v. 84, p. GP41C-0053 F554.

Jennings, A. Dunhill, G. Stoner, J. S. & Andrews, J. T., 2003, Paleomagnetic Calibration of Radiocarbon Chronologies: Synchronization of High-Resolution Holocene Marine Sediment Records Between North Iceland and East Greenland. Eos. Trans. AGU, 84(46) Fall Meet. Suppl., Abstract PP42A-0869.

Karig, D. E., Lawrence, M. B., Moore, G. F., and Curray, J. R., 1980, Structural framework of the forearc basin, NW Sumatra: Geol. Soc. London Jour., v. v. 137, p. p. 77-91.

Karlin, R.E., Holmes, M., Abella, S.E.B., and Sylwester, R., 2004, Holocene landslides and a 3500-year record of Pacific Northwest earthquakes from sediments in Lake Washington: Geological Society of America Bulletin, v. 116, p. 94-108.

Karig, D. E. Lawrence, M. B., Moore, G. E. & Curray, J. R., (1980), Structural framework of the fore-arc basin, NW Sumatra. J. geol. Soc. London 137, 77-91.

Kopf, A., and Brown, K.M., (2003), Friction experiments on saturated sediments and their implications for the stress state of the Nankai and Barbados subduction thrusts: Marine Geology, v. 202, p. 193-210.

Kotilainen, A. T., Saarinen, T., and Winterhalter, B. High-resolution paleomagnetic dating of sediments deposited in the central Baltic Sea during the last 3000 years. *Marine Geology*, 166, 51-64 (2000).

Korte, M., and Constable, C., 2003, Continuous global geomagnetic field models for the past 3000 years, Phys. Earth. Planet. Inter. 140, 73-89.

Kumon, F., Inouchi, Y., Shiki, T., Nakano, S., and Yasumatsu, S., 1998, Seismic turbidites in Lake Biwa, Japan, *in* Canaveras, J.C., Garcia del Cura, M.A., Soria, J., Melendez Hevia, A., and Soria, A.R., eds., 15th international sedimentological congress; sedimentology at the dawn of the third millennium; abstracts: (1998), Publisher Univ. Alicante, Alicante, Spain, p. 486-487.

Ladage, S., C. Gaedicke, U. Barckhausen, I. Heyde, W. Weinrebe, E. R. Flueh, A. Krabbenhoeft, H. Kopp, S. Fajar, and Y. Djajadihardja (2006), Bathymetric Survey Images Structure off Sumatra, *Eos Trans. AGU*, 87(17), 165.

Laj, C., C Kissel, A. Mazaud, J.E.T. Channell and J. Beer, 2000, North Atlantic PaleoIntensity Stack since 75 ka (NAPIS-75) and the duration of the Laschamp event. Phil. Trans. R. Soc. Series A. 1009-1025.

Lallemand, S. E., P. Schnürle, and J. Malavieille, (1994), Coulomb theory applied to accretionary and nonaccretionary wedges: Possible causes for tectonic erosion and/or frontal accretion, J. Geophys. Res., 99 (B6), 12,033-12,055.

Lohrmann, J., N. Kukowski, J. Adam, and O. Oncken, (2003), The impact of analogue material properties on the geometry, kinematics, and dynamics of convergent sand wedges, J. Struct. Geol., 25, 1,691-1,711.

Lund, S, Stoner, J. Klevien, H., Ninnemann, U., Lamy, F. & J. McManus, 2003, Late Quaternary Records of Magnetic Field Excursions from the Southern Hemisphere (ODP Leg 202 - Chilean Margin). Eos. Trans. AGU, 84(46) Fall Meet. Suppl., Abstract GP31D-0771.

Lund, S. P., 1996, A comparison of paleomagnetic secular variation records from North America. J. Geophys. Res., 101, 8007-24.

Lund, S. P., and Schwartz, M.,Paleomagnetic secular variation as a high-resolution chronostratigraphic tool in Quaternary paleoclimatic studies of lacustrine and deep-sea sediments, GSA Annual Meeting Abstracts, 28, A-232, (1996).

MacKay, M. E., Moore, G. F., Cochrane, G. R., Moore, J. C., and Kulm, L. D., 1992, Landward vergence and oblique structural trends in the Oregon margin accretionary prism: Implications and effect on fluid flow: Earth and Planet. Sci. Lett., v. 109, p. 477-491.

MacKay, M.E., (1995), Structural variation and landward vergence at the toe of the Oregon accretionary prism: Tectonics, v. 14, p. 1309-1320.

Mandal, N., A. Chattopadhyay, and S. Bose, (1997), Imbricate thrust spacing: Experimental and theoretical analyses, in Evolution of geological structures in micro- to macro-scales, edited by S. Sengupta, Chapter 8.1, Chapman and Hall, London.

Marone, C., and C.H. Scholz, (1988), The depth of seismic faulting and the upper transition from stable to unstable regimes, Geophysical Research Letters, 15, pp.621-624.

Marone, C., and Saffer, D.M., 2006, Fault friction and the upper transition from seismic to aseismic faulting, in press, in The seismogenic Zone of Subduction Thrusts, edited by T. Dixon et al., Columbia University Press.

Martin-Barajas, A. and Lallier-Vergas, E., *Mar. Geol.*, 1993, 115, 307–329.

Mazaud, A., Sicre, M. A., Ezat, U., Pichon, J. J., Duprat, J., Laj, C., Kissel, C., Beaufort, L., Michel. E., Turon, J. L., 2002, Geomagnetic-assisted stratigraphy and sea surface temperature changes in core MD94-103 (Southern Indian Ocean): possible implications for North-South climatic relationships around H4. Earth Planet. Sci. Lett, 201, 159-170.

McCaffrey, R., 1991, Slip vectors and stretching of the Sumatran forearc: Geology, v. 19, p. 881-884.

Moore, D. G., Curray, J., and Emmel, F. J., 1976, Large Submarine slide (olistostrome) associated with Sunda Arc subduction zone, northeast Indian Ocean: Marine Geology, v. 21, p. 211-226.

Moore, D. E., and D. A. Lockner, (2005), Friction of the smectite clay montmorillonite: A review and interpretation of data, in The Seismogenic Zone of Subduction Thrust Faults, edited by T. Dixon and J. C. Moore, Columbia University Press, in press.

Moore, J. C., and D. Saffer, (2001), Updip limit of the seismogenic zone beneath the accretionary prism of southwest Japan: An effect of diagenetic to low grade metamorphic processes and increasing effective stress, Geology, 29, 183-186.

Morey-Ross, A., Goldfinger, C., Nelson, C.H., Chaytor, J., Johnson, J.E., Ericsson, E., and the shipboard scientific party, 2003, Turbidite Based Earthquake Record Along the Northern San Andreas Fault: Eos, Transactions of the American Geophysical Union.

Mulder, T., and Syvitsky, J.M., 1995, Turbidity currents generated at river mouths during exceptional discharges to the world oceans: Journal of Geology, v. 103, p. 285-299.

Nakajima, T., 2000, Initiation processes of turbidity currents; implications for assessments of recurrence intervals of offshore earthquakes using turbidites: Bulletin of the Geological Survey of Japan, v. 51, p. 79-87.

Nakajima, T., and Kanai, Y., 2000, Sedimentary features of seismoturbidites triggered by he 1983 and older historical earthquakes in the easterrn margin of the Japan Sea: Sedimentary Geology, v. 135, p. 1-19.

Nakajima, T., 2004, Earthquake potential north of Sao Ridge, Japan Sea, inferred from turbidites, *in* Satake, K., Goldfinger, C., ed., Workshop on Turbidites as Earthquake Recorders: Tsukuba, Japan, AIST, Geological Survey of Japan.

Natawidjaja, D. H., Sieh, K., Ward, S. N., Cheng, H., Edwards, R. L., Galetzka, J., and Suwargadi, B. W., 2003, Paleogeodetic records of seismic and aseismic subduction from central Sumatran microatolls, Indonesia: Journal of Geophysical Research, v. 109, p. doi:10.1029/2003JB002398.

Natawidjaja, D. H., Sieh, K., Ward, S. N., Cheng, H., Edwards, R. L., Galetzka, J., and Suwargadi, B. W., 2004, Paleogeodetic records of seismic and aseismic subduction from central Sumatran microatolls, Indonesia: Journal of Geophysical Research, v. 109, p. doi:1029/2003JB002398.

Neff U., S. J. Burns, A. Mangini, M. Mudelsee, D. Fleitmann & A. Matter, 2001, Strong coherence between solar variability and the monsoon in Oman between 9 and 6 kyr ago Nature, 411, 290-293.

Nelson, A.R., Atwater, B.F., Brobowski, P.T., Bradley, L.A., Clague, J.J., Carver, G.A., Darienzo, M.E., Grant, W.C., Krueger, H.W., Sparks, R., Stafford, T.W., and Stuiver, M., 1995, Radiocarbon evidence for extensive plate-boundary rupture about 300 years ago at the Cascadia subduction zone: v. 378, p. 371-374.

Nelson, C.H., 1968, Marine Geology of Astoria Deep-Sea Fan: Ph.D. Thesis, Corvallis, Oregon State University, 289 p.

Nelson, C.H., Kulm, L.D., Carlson, P.R., and Duncan, J.R., 1968, Mazama ash in the northeastern Pacific: Science, v. 161, p. 47-49.

Nelson, C.H., 1976, Late Pleistocene and Holocene depositional trends, processes, and history of Astoria Deep-Sea Fan, northeast Pacific: Marine Geology, v. 20, p. 129-173.

Nelson, C. H., Goldfinger, C. Vallier, T.L. McGann, M.L., Kashgarian, M., l996, North to south variation in Cascadia Basin turbidite event history: implications for paleoseismicity, Geological Society of America Abstracts with Programs, 28(5): 95.

Nelson, C.H., and Maldonado, A., 1988, Factors controlling depositional patterns of Ebro turbidite systems, Mediterranean Sea: Am. Assoc. Petrol. Geol. Bull., v. 72, p. 698-716.

Nelson, C.H., and Nilsen, T.H., 1984, Modern and ancient deep-sea fan sedimentation: Society of Econ. Geol. and Paleo. Short Course, Tulsa OK, no. 14, 403 p.

Nelson, C.H., B. Savoye , J.P. Rehault and C. Escutia, 1995, Interfingering of western Corsican margin aprons with the Var Fan lobe and an apparent Late Quaternary Corsican paleoseismic event, International Association of Sedimentologists 16th Regional European Meeting, Aix-les-Bains, Savoie, France, Abstracts Volume, p. 113.

Nelson, C.H., Twichell, D.C., Schwab, W.C., Lee, H.J., and Kenyon, N.H., 1992, Upper Pleistocene turbidite sand beds and chaotic silt beds in the channelized, distal, outer-fan lobes of the Mississippi Fan: Geology, v. 20, p. 693-696.

Nelson, C. H., Chris Goldfinger, Joel E. Johnson , Gita Dunhill , 2000a, Variation of Modern Turbidite Systems Along the Subduction Zone Margin of Cascadia Basin and Implications for Turbidite Reservoir Beds, in Weimer, P.W., Nelson, C. H. et al. (Editors), Deep-water Reservoirs of the World, Gulf Coast Section Society of Economic Paleontologists and Mineralogists Foundation 20th Annual Research Conference, Dec.3, 2000, Houston, TX., 31p, 15 Figures.

Nelson, C.H., Goldfinger, C., and Johnson, J.E., 2000b, Turbidite event stratigraphy: Implications for Holocene paleoseismicity of the Cascadia Subduction Zone and northern San Andreas Faults: EOS, Transactions of the American Geophysical Union, v. 81, p. F851.

Noda, A., 2004, Turbidites along Kushiro Canyon, *in* Satake, K., Goldfinger, C., ed., Workshop on Turbidites as Earthquake Recorders: Tsukuba, Japan, AIST, Geological Survey of Japan.

Ojala, A. E. K, and M. Tiljander. Testing the fidelity of sediment chronology: comparison of varve and paleomagnetic results from Holocene lake sediments from central Finland. *Quaternary Science Reviews* 22, 1787-1803 (2003).

Okamura, Y., 2004, Paleoseismology of deep-sea faults based on marine surveys in Japan Sea, *in* Satake, K., Goldfinger, C., ed., Workshop on Turbidites as Earthquake Recorders: Tsukuba, Japan, AIST, Geological Survey of Japan.

Oleskevich, D. A., R. D. Hyndman, and K. Wang, (1999), The updip and downdip limits to great subduction zone earthquakes: Thermal and structural models of Cascadia, South Alaska, SW Japan, and Chile, J. Geophys. Res., 104, 14,956-14,991.

Pal, T., Chakraborty, P. P., Gupta, T. G., and Singh, C. D., 2003, Geodynamic evolution of the outer-arc–forearc belt in the Andaman Islands, the central part of the Burma–Java subduction complex: Geology Magazine, v. 140, no. 3, p. 289-307.

Pattan, J. N., Pearce, N. J. G., Banakar, V. K., and Parthiban, G., 2002, Origin of ash in the Central Indian Ocean Basin and its implication for the volume estimate of the 74,000 year BP Youngest Toba eruption: Current Science, v. 83, no. 7, p. 889-893.

Pattan, J. N., Shane, P. and Banakar, V. K., *ibid*, 1999, 155, 243–248.

Pilkey, O.H., 1988, Basin plains; Giant sedimentation events: Geological Society of America Special Paper, 229, 93-99.

Prentice, C.S., 1989, Earthquake Geology of the Northern San Andreas Fault near Point Arena, California [PhD Thesis]: California Institute of Technology.

Prawirodirdjo, L., Y. Bock, R. McCaffrey, J. Genrich, E. Calais, C. Stevens, S. S. O. Puntodewo, C. Subarya, and J. Rais, 1997, Geodetic observations of interseismic strain segmentation at the Sumatra subduction zone, Geophysical Research Letters, 2601-2604.

Prell, W., Martin, A., Cullen, J. and Trend, M., 1999, The Brown University Foraminiferal Data Base, IGBP PAGES/World Data Center-A for Paleoclimatology Data Contribution Series # 1999-027. NOAA/NGDC Paleoclimatology Program, Boulder CO, USA.

Saffer, D.M., and Bekins, B.A., (1999), Fluid budgets at convergent plate margins: Implications for the extent and duration of fault-zone dilation: Geology, v. 27, p. 1095-1098.

Saffer, D. M., and B. A. Bekins, (2002), Hydrologic controls on the morphology and mechanics of accretionary wedges, Geology, 30, 271-274.

Satake, K., Shimazaki, K., Tsuji, Y., and Ueda, K., 1996, Time and size of a giant earthquake in Cascadia inferred from Japanese tsunami records of January, 1700: Nature, v. 379, p. 246-249.

Schnellmann, M., Anselmetti, F.S., Giardini, D., McKenzie, J.A., and Ward, S.N., 2002, Prehistoric earthquake history revealed by lacustrine slump deposits: Geology (Boulder), v. 30, p. 1131-1134.

Scholz, C. H., (2003), The Mechanics of Earthquakes and Faulting (2nd Edition), Cambridge University Press, Cambridge, 471 p.

Schwartz, D. P., Pantosti, D., Okumura, K., Powers, T. J., and Hamilton, J. C., 1998, Paleoseismic investigations in the Santa Cruz mountains, California: Implications for recurrence of large-magnitude earthquakes on the San Andreas fault: Journal of Geophysical Research, vol., 103, no. 8, p. 17985-18001.

Seely, D. R., 1977, The significance of landward vergence and oblique structural trends on trench inner slopes, *in* M. Talwani and W.C. Pitman, I., ed., Island Arcs, Deep Sea Trenches and Back-Arc Basins: Maurice Ewing Series I: Washington, D.C., Am. Geophy. Un., p. 187-198.

Shanmugan, G., and Moiola, R.J., 1988, Submarine fans: Characteristics, models, classification, and reservoir potential, Earth-Science Reviews, v. 24, p. 383-428.

Schulte, S., and Bard, E., 2003, Past changes in biologically mediated dissolution of calcite above the chemical lysocline recorded in Indian Ocean sediments: Quaternary Science Reviews, v. 22, p. 1757–1770.

Shiki, T., Cita, M.B., and Gorsline, D.S., 2000a, Sedimentary features of seismites, seismo-turbidites and tsunamiites – an introduction: Sedimentary Geology, v. 135, p. vii-ix.

Shiki, T., Kumon, F., Inouchi, Y., Kontani, Y., Sakamoto, T., Tateishi, M., Matsubara, H., and Fukuyama, K., 2000b, Sedimentary features of the seismo-turbidites, Lake Biwa, Japan: Sedimentary Geology, v. 135, p. 37-50.

Sieh, K., and D. Natawidjaja, Neotectonics of the Sumatran fault, Indonesia, J. Geophys. Res., 105, 28,295– 28,326, 2000.

Skinner, L. C., and McCave, I. N., 2003, Analysis and modeling of gravity- and piston coring based on soil mechanics: Marine Geology, v. 199, p. 181-204.

Smoot, J.P., Litwin, R.J., Bischoff, J.L., and Lund, S.J., 2000, Sedimentary record of the 1872 earthquake and "Tsunami" at Owens Lake, southeast California: Sedimentary Geology, v. 135, p. 241-254.

Song, T.-R. A., and Simons, M., (2003), Large Trench-Parallel Gravity Variations Predict Seismogenic Behavior in Subduction Zones: Science, v. 301, p. 630-633.

Southon, J.R., Nelson, D.E., and Vogel, J.S., 1990, A record of past ocean-atmosphere radiocarbon differences from the Northeast Pacific, Paleoceanography, v. 5, no. 2, p. 197-206.

Soh, W., 2004, Coseismic seafloor displacement along Enshu fault detected from NSS coring, in Satake, K., Goldfinger, C., ed., Workshop on Turbidites as Earthquake Recorders: Tsukuba, Japan, AIST, Geological Survey of Japan.

Southon, J.R., Nelson, D.E., and Vogel, J.S., 1990, A record of past ocean-atmosphere radiocarbon differences from the Northeast Pacific, Paleoceanography, v. 5, no. 2, p. 197-206.

Sternberg, R. W., 1986, Transport and accumulation of river-derived sediment on the Washington continental shelf, USA, Jour. of Geol. Soc. London, v. 143, p 945-956.

St-Onge, G., J. S. Stoner & C. Hillaire-Marcel, 2003, Holocene paleomagnetic records from the St. Lawrence Estuary, Eastern Canada: centennial to millennial-scale geomagnetic modulation of cosmogenic isotopes. Earth and Planetary Science Letters, 209, 113-130 ().

Stoner, J. S., J. E. T. Channell, D. A. Hodell & C. D. Charles, 2003a, A ~ 580 kyr paleomagnetic record from the sub-Antarctic South Atlantic (ODP Site 1089). Journal of Geophysical Research, 108(B5) 2244, doi:10,1029/2001JB001390.

Stoner, J.S., Channell, J.E.T., and Hillaire-Marcel, C. The magnetic signature of rapidly deposited detrital layers from the deep Labrador Sea: relationship to North Atlantic Heinrich layers. Paleoceanography, 11:309–325 (1996).

Stoner, J. S., and Andrews, J. T. The North Atlantic as a Quaternary magnetic archive. In Quaternary climates, environments and magnetism, ed. B. A. Maher and R. Thompson, pp. 49-80, Cambridge, Cambridge University press (1999).

Stoner, J.S., Channell, J.E.T., Hillaire-Marcel, C., and Kissel, C., 2000. Geomagnetic paleointensity and environmental record from Labrador Sea Core MD95-2024: global marine sediment and ice core chronostratigraphy for the last 110 kyr. Earth Planet. Sci. Lett., 183:161–177.

Stoner, J. S., G. B. Kristjansdottir, A. E. Jennings, J. T. Andrews, J. Hardardottir & G. Dunhill. Developing a Holocene Chronostratigraphic Template for the North Atlantic: Paleomagnetic, Radiocarbon and Tephra Chronostratigraphies from Iceland (MD99-2269) and East Greenland (MD99-2322). *Eos. Trans. AGU*, 85(47) Fall Meeting Suppl., Abstract GP43B-0851, (2004)

Stoner, J. S., Jennings, A., Kristjansdottir, G. B., Andrews, J. T., Hardadottir, J., & Dunhill, G. Paleomagnetic approach toward refining radiocarbon based chronologies and stratigraphy: Centennial scale phase relations of paleoceanographic records from North Iceland (MD99-2269) and East Greenland (MD99-2322). In prep.

St-Onge, G., D. J. W. Piper, T. Mulder, C. Hillaire-Marcel & J. S. Stoner, 2004, Earthquake and flood-induced turbidites in the Saguenay Fjord (Québec): a Holocene paleoseismicity record. Quaternary Science Reviews, 23, 283-294.

Stuvier, M., and Braziunas, T.F., 1993, Modeling atmospheric 14C influences and 14C ages of marine samples to 10,000 BC: Radiocarbon, v. 35, p. 137-189.

Stuvier, M., Reimer, P.J., Bard, E., Beck, J.W., Burr, G.S., Hughen, K.A., Kromer, B., McCormack, F.G., Plicht, J., and Spurk, M., 1998, INTCAL98 Radiocarbon age calibration 24,000 - 0 cal BP: Radiocarbon, v. 40, p. 1041-1083.

Sugiyama, Y., 1994, Neotectonics of Southwest Japan due to the right-oblique subduction of the Philippine Sea plate: Geofisica Internacional, v. 33, p. 53-76..

Thomson, J., and Weaver, P.P.E., 1994, An AMS radiocarbon method to determine the emplacement time of recent deep-sea turbidites, Sed. Geol., v. 89, p. 1-7.

Thompson, R. Palaeolimnology and paleomagnetism. Nature 242, 182-184 (1973).

Thompson, R. A global review of paleomagnetic results from wet lake sediments. Pp. 145-165 in Haworth, E. Y. and Lund, J. W. G (eds): *Lake sediments and Environmental History*. University of Minnesota Press, Minneapolis, (1984).

Thompson, R. and Turner, G. M. British geomagnetic master curve 10,000-0yr. B.P. of dating European sediments, *Geophys. Res. Lett.,* 6, 249-252 (1979)

Toda, S., Stein, R.S., and Sagiya, T., 2002, Evidence from the AD 2000 Izu Islands earthquake swarm that stressing rate governs seismicity: Nature (London), v. 419, p. 58-61.

Tucker, M. E., and P. V. Wright, P. V., 1990, Carbonate Sedimentology: Oxford, Blackwell Science.

Verosub, K. L., Mehringer Jr. P. J., and Waterstraat, P. Holocene secular variation in western North America: Paleomagnetic record from Fish Lake, Harney County, Oregon, *J. Geophys. Res.*, 91, 3609-3623, (1986)

Verosub, K. L., Harris A. H., and Karlin, R. Ultra high-resolution paleomagnetic record from ODP Leg 169S, Saanich Inlet, British Columbia: intial results. *Marine Geology*, 79-93, 174 (2001).

Vigny, C., W. J. F. Simons, et al., (2005), "Insight into the 2004 Sumatra–Andaman earthquake from GPS measurements in southeast Asia." Nature 436: 201-206.

Von Huene, R., and D. Klaeschen, (1999), Opposing gradients of permanent strain in the aseismic zone and elastic strain across the seismogenic zone of the Kodiak shelf and slope, Alaska, Tectonics, 18, 248-262.

Wang, K., and Hu, Y., (2006), Accretionary prisms in subduction earthquake cycles: The theory of dynamic Coulomb wedge, Journal of Geophysical Research, v.111, B06410.

Weeks, R., Laj, C., Endignoux, L., Fuller, M., Roberts, A., Manganne, R., Blanchard, E., and Goree, W., 1993. Improvements in long-core measurement techniques: applications in palaeomagnetism and palaeoceanography. Geophys. J. Int. 114, 651-662.

Wiedecke-Hombach, M., Ardhayastuti, S., Bruns, A., Delisle, R., Goergens, T., Hermawan, T., Kanamatsu, T., Luckge, A., Mohtadi, M., Muhr, P., Rahadyan, R., Riyadi, A., Ruhlemann, C., Schippers, A., Schlomer, S., Taufik, Teichert, B., Vink, A., Weiss, W., Wijaya, H., Wohrl, C., Seibig, M., and Zoch, D., (2006), Cruise Report, SO189-2, Sumatra, the hydrocarbon system of the Sumatra forearc: Hanover, BGR, 215 p.

Wells, R. E., R. J. Blakely, Y. Sugiyama, D. W. Scholl, and P. A. Dinterman, (2003), Basin-centered asperities in great subduction zone earthquakes: A link between slip, subsidence, and subduction erosion? J. Geophys. Res., 108(B10), doi:10.1029/2002JB002072.

Wynn, R. B., Weaver, P. P. E., Masson, D. G., and Stow, D. A. V., 2002, Turbidite depositional architecture across three interconnected deep-water basins on the north-west African margin: Sedimentology, v. 49, no. 4, p. 669-695.

Zdanowicz, C.M., Zielinski, G.A., and Germani, M.S., 1999, Mount Mazama eruption: Calendrical age verified and atmospheric impact assessed: Geology, v. 27, p. 621-624.

References for Cascadia land paleoseismic event ages shown in Figure 5.

Atwater, B. F., and Hemphill-Haley, E., 1997, Recurrence intervals for great earthquakes of the past 3500 years at northeastern Willapa Bay, Washington: U.S. Geological Survey Professional Paper, v. 1576, p. 108 p.

Clague, J.J., Bobrowsky, P.T., and Hutchinson, I., 2000, A review of geological records of large tsunamis at Vancouver Island, British Columbia, and implications for hazard: Quaternary Science Reviews, v. 19, p. 849-863.

Clague, J.J., Hutchinson, I., Mathewes, R.W., and Patterson, R.T., 1999, Evidence for late holocene tsunamis at Catala Lake, British Columbia: Journal of Coastal Research, v. 15, p. 45-60.

Clarke Jr., S. H., and Carver, G. A., 1992, Late Holocene tectonics and paleoseismicity, southern Cascadia subduction zone: Science, v. vol. 255, p. pp. 188-191.

Darienzo, M. E., and Peterson, C. D., 1990, Episodic tectonic subsidence of late Holocene salt marshes, northern Oregon central Cascadia margin: Tectonics, v. 9, p. 1-22.

-, 1995, Magnitude and frequency of subduction-zone earthquakes along the northern Oregon coast in the past 3,000 years: Oregon Geology, v. 57, no. 1, p. 3-12.

Darienzo, M. E., Peterson, C. D., and Clough, C., 1994, Stratigraphic evidence for great subduction-zone earthquakes at four estuaries in northern Oregon, U.S.A.: Journal of Coastal Research, v. v. 10, no. no. 4, p. p. 850-876.

Garrison-Laney, C. E., Abramson, H. F., and Carver, G. A., 2002, Late Holocene tsunamis near the southern end of the Cascadia Subduction Zone: Seismological Research Letters, v. 73, no. 2, p. 248.

Hutchinson, I., Clague, J.J., Bobrowsky, P.T., and Williams, H.F.L., 2000, Investigations of Cascadia paleoseismicity in southwestern BC and northern most Washington State: Special Paper - Oregon, Department of Geology and Mineral Industries, p. 61.

Kelsey, H. M., Nelson, A. R., Hemphill-Haley, E., and Witter, R. C., 2004, Tsunami history of an Oregon coastal lake reveals a 4,600 year record of great earthquakes on the Cascadia subduction zone: Geological Society of America Bulletin, v. in press.

Kelsey, H. M., Witter, R. C., and Hemphill-Haley, E., 1998, Response of a small Oregon estuary to coseismic subsidence and postseismic uplift in the past 300 years: Geology, v. 26, p. 231-234.

-, 2002, Plate-boundary earthquakes and tsunamis of the past 5500 yr, Sixes River estuary, southern Oregon: Geological Society of America Bulletin, v. 114, no. 3, p. 298-314.

Lees, J. A., Fowler, R. J., and Appleby, P. G., 1998, Mineral magnetic and physical properties of surficial sediments and onshore samples from the southern basin of Lake Baikal, Siberia: Journal of Paleolimnology, v. 20, no. 2, p. 175-186.

Meyers, R. A., Smith, D. G., Jol, H. M., and Peterson, C. D., 1996, Evidence for eight great earthquake-subsidence events detected with ground-penetrating radar, Willapa barrier, Washington: Geology, v. 24, no. 2, p. 99-102.

Nelson, A. R., 1992, Discordant 14C ages from buried tidal marsh soils in the Cascadia Subduction zone, southern Oregon coast: Quat. Res., v. v. 38, p. 74-90.

-, 1992, Holocene tidal-Marsh Stratigraphy in South-Central Oregon-Evidence for Localized Sudden Submergence in the Cascadia Subduction Zone, *in* Fletcher, C. H., and Wehmiller, J. F., eds., Quaternary Coasts of the United States: Marine and Lacustrine Systems, Society for Sedimentary Geology Special Publication, p. p. 287-301.

Nelson, A. R., Atwater, B. F., Brobowski, P. T., Bradley, L. A., Clague, J. J., Carver, G. A., Darienzo, M. E., Grant, W. C., Krueger, H. W., Sparks, R., Stafford, T. W., and Stuiver, M., 1995, Radiocarbon evidence for extensive plate-boundary rupture about 300 years ago at the Cascadia subduction zone: Nature, v. v. 378, p. p. 371-374.

Nelson, A. R., Jennings, A. E., and Kashima, K., 1996, An earthquake history derived from stratigraphic and microfossil evidence of relative sea-level change at Coos Bay, southern coastal Oregon: GSA Bull., v. v. 108, no. no. 2, p. p. 141-154.

Nelson, A. R., Kelsey, H. M., Hemphill-Haley, E., and Witter, R. C., 2000, Oxcal analyses and varve-based sedimentation rates constrain the times of 14C dated tsunamis in Southern Oregon, *in* Penrose Conference 2000 Great Cascadia Earthquake Tricentenial, Seaside, Oregon, pp. 87.

Nelson, A. R., and Personius, S. F., 1996, Great-earthquake potential in Oregon and Washington - an overview of recent coastal geologic studies and their bearing on segmentation of Holocene ruptures, central Cascadia subduction zone, *in* Rogers, A. M., Walsh, T. J., Kockelman, W. J., and Priest, G., eds., Assessing and reducing earthquake hazards in the Pacific Northwest, U.S. Geological Survey, p. 91-114.

Nelson, A. R., Personius, S. F., and Rhea, S., 1988, Earthquake recurrence and Quaternary deformation in the Cascadia subduction zone, coastal Oregon: U.S. Geological Survey, 88-673.

Nelson, C. H., Goldfinger, C., Vallier, T. L., McGann, M. L., and Kashgarian, M., 1996, North to south variation in Cascadia Basin turbidite event history: implications for paleoseismicity: Geological Society of America Abstracts with Programs, v. v. 28, no. no. 5, p. p. 96.

Peterson, C. D., Darienzo, M. E., Burns, S. F., and Burris, W. K., 1993, Field trip guide to Cascadia paleoseismic evidence along the northern Oregon coast: Evidence of subduction zone seismicity in the central Cascadia margin: Oregon Geology, v. 55, p. 99-114.

Peterson, C. D., and Priest, G. R., 1995, Preliminary reconnaissance survey of Cascadia paleotsunami deposits in Yaquina Bay, Oregon: Oregon Geology, v. 57, p. 33-40.

Witter, R. C., Kelsey, H. M., and Hemphill-Haley, E., 2003, Great Cascadia earthquakes and tsunamis of the past 6700 years, Coquille River estuary, southern coastal Oregon: Bulletin of the Geological Society of America, v. 115, no. 10, p. pp. 1289–1306.

This Page Intentionally
Left Blank